

Autoionization widths for $\text{Ne}^*(3s)\text{-Ar}$ and $\text{Ne}^{**}(3p)\text{-Ar}$ collisions

J. P. J. Driessen,* S. S. Op de Beek, L. M. T. Somers, H. C. W. Beijerinck, and B. J. Verhaar
Physics Department, Eindhoven University of Technology, P.O. Box 513, 5600 MB Eindhoven, The Netherlands

(Received 26 March 1990; revised manuscript received 21 January 1991)

Following Jones and Dahler [Phys. Rev. A **37**, 2916 (1988)] we study the theory of the process of ionization within the framework of the Feshbach projection-operator formalism, with the discrete fine-structure states (before ionization) and the continuum states (after ionization) as the two separate subspaces of Hilbert space. For the $\text{Ne}^*(3s)\text{-Ar}$ and $\text{Ne}^{**}(3p)\text{-Ar}$ systems we have calculated *ab initio* autoionization widths. In the approximation in which only two electrons play an active role, the coupling matrix element between the two subspaces is a linear combination of two-center two-electron integrals for the exchange and the radiative mechanisms. In general, our calculations support the semiempirical results of Morgner [J. Phys. B **18**, 251 (1985)] for the coupling matrix elements as derived from experimental data. The autoionization widths $\Gamma_{J',J\Omega}$ are presented for initial states $|J,\Omega\rangle$ of the $\text{Ne}^{*(*)}$ atom and final states $|J'\rangle$ of the Ar^+ ion. They show a pronounced Ω dependence and a strong correlation of initial and final states, e.g., $|0,0\rangle \rightarrow |3/2\rangle$ and $|2,2\rangle \rightarrow |3/2\rangle$. For the $\text{Ne}^*(3s)$ states the two-center two-electron calculation is in good agreement with the two-state basis of Driessen *et al.* [Phys. Rev. A **42**, 4058 (1990)], based on a one-electron overlap approximation. In a semiclassical model the polarized-atom ionization cross sections are calculated. For the $\text{Ne}^{**}(3p)\text{-Ar}$ system the energy dependence of both the polarization effect and the average cross-section value is reproduced very well, in contrast to the one-electron approximation. For the $\text{Ne}^*(3s)\text{-Ar}$ system we have to conclude that the *ab initio* results cannot explain all experimental observed features, such as the large cross-section ratio $Q(^3P_0)/Q(^3P_2)$.

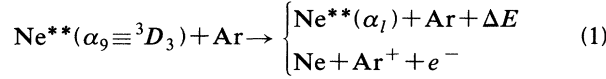
I. INTRODUCTION

In the past 15 years Penning ionization has been investigated in detail by many groups, for a variety of metastable and short-lived electronically excited projectiles, and an even larger number of target atoms and molecules.¹⁻²¹ In crossed-beam experiments with time-of-flight analysis of the primary beam the energy dependence of the ionization cross section can be studied very accurately.^{16-18,20} More detailed results can be obtained since the availability of stabilized cw single-mode dye lasers. State-selected measurements with metastable rare-gas atoms have been performed extensively.^{16,18} Recently the point of interest has shifted to collision experiments with polarized laser-excited atoms.^{11-14,19-21} In view of the large effort one would expect to find a mature field without unsolved basic problems. However, this is not true. Although a large amount of insight has been obtained, some very fundamental problems have not been solved as yet. A striking example is the ionization cross section for the $\text{Ne}^*[(3s);^3P_{0,2}]\text{-Ar}$ system,^{7,15,16} where at thermal energies $0.05 \text{ eV} \leq E \leq 0.2 \text{ eV}$ the $\text{Ne}^*(^3P_0)$ state has a 30% larger cross section, increasing to 80% in the superthermal energy range $1 \text{ eV} \leq E \leq 5 \text{ eV}$. Despite all experimental and theoretical effort it has not been decided whether differences in the real or the imaginary part of the optical potential are responsible for this effect. It is generally accepted that the difference in the real potential $V(R)$ for the two $\text{Ne}^*[(3s);^3P_{0,2}]$ states is negligible.²² A difference in the imaginary part, the so-called autoionization width, seems to be obvious. However, there is no mathematical evidence for such a difference in the spheri-

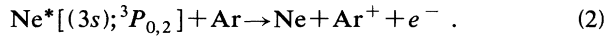
cally averaged autoionization width as yet, as discussed by Driessen *et al.*²¹ This does not imply that the ionization cross section $Q(J=2)$ for unpolarized $\text{Ne}^*[(3s);^3P_2]$ atoms is equal to that of $\text{Ne}^*[(3s);^3P_0]$ atoms: the full dynamics of the collision, which is essentially nonlinear in the Ω -dependent autoionization widths, enters this last step. Experimental results for state-selected ionization cross sections are usually described in an empirical fashion, using the *ad hoc* assumption of different autoionization widths.¹⁶ To avoid this *ad hoc* step, Hausmann²³ has investigated the influence of small differences in the shape of the real part of the potential, while keeping the autoionization width fixed. This approach also cannot explain the experimentally observed, large $Q(J=0)/Q(J=2)$ ratio.

The $\text{Ne}^*(2p)^5(3s)$ multiplet contains two metastable states $^3P_0, ^3P_2$ from which the $\text{Ne}^{**}(3p)$ states can be excited. Typical lifetimes of the $\alpha_i \equiv [(2p)^5(3p)]_i$ states, with i running from 1 to 10 with decreasing energy, are $\tau \approx 20 \text{ ns}$. We will concentrate on the metastable $\text{Ne}^*[(2p)^5(3s);^3P_{0,2}]$ and the laser-excited $\text{Ne}^{**}[(2p)^5(3p);^3D_3 \equiv \alpha_9]$ atoms colliding with Ar, for which cross-section data are available in a wide energy range.^{11-13,20,21} The polarized-atom cross section $^JQ^{M|}(E)$ refers to the collision of the target atom with an asymptotic pure magnetic substate $\text{Ne}^{*(*)}(|J,M\rangle_g)$ with respect to the initial relative velocity \mathbf{g} . The $\text{Ne}^{**}(^3D_3)$ state constitutes a two-level system with the metastable $\text{Ne}^*(^3P_2)$ state and can be excited repeatedly, making energy-resolved experiments possible. For a later purpose we stress that only triplet states are involved in the experiment.

In the analysis of the ionization process we have to take into account all possible inelastic channels. For $\text{Ne}^{**}(\alpha_i)\text{-Ar}$ collisions the competing inelastic channels besides ionization are fine-structure changing collisions.^{24,25} We thus have



∥



Of course, associative ionization with $(\text{NeAr})^+$ ions can also occur. Although a large number of molecular states $|J, \Omega\rangle$ is involved, the potentials $V(R)$ can be determined through the model potential method^{24,26,27} as a linear combination of two elementary potentials $V_\sigma(R)$ and $V_\pi(R)$ for the $|(3p); |m_l|=0,1\rangle$ states of the valence electron. The additional anisotropic interaction, due to the oriented $\text{Ne}^+(2p)^{-1}$ hole, becomes noticeable only at short internuclear distances R and can similarly be described by linearly combining the elementary potentials $V_\sigma(R)$ and $V_{\pi'}(R)$.^{24,28} For the $\text{Ne}^*(3s)\text{-Ar}$ system only the core potentials $V_{\sigma'}(R)$ and $V_{\pi'}(R)$ give an anisotropic contribution. For the internuclear distances R probed in thermal energy collisions, this potential splitting is negligible and the same $\text{Ne}^*(3s)\text{-Ar}$ potential is used for all molecular states $|J, \Omega\rangle$.

The ionization process is usually described by an optical potential $V_{\text{opt}}(R)$ given by²⁹

$$V_{\text{opt}}(R) = V(R) - \frac{1}{2}i\Gamma(R) . \quad (3)$$

In a classical interpretation the real part $V(R)$ determines the classical trajectories and the autoionization width $\Gamma(R)$ takes into account the loss of flux due to ionization. The ionization rate at an internuclear distance R is equal to $\Gamma(R)/\hbar$. To determine the R dependence of the width $\Gamma(R)$ of the optical potential, we have to obtain insight into the mechanism of the process of ionization. Two mechanisms have been proposed:^{8,29,30} a *radiative* mechanism and an *exchange* mechanism. In the *radiative* mechanism the excited $\text{Ne}^{**}(\alpha_i)$ state decays to the ground state, accompanied by the promotion of an electron of the target atom to a free-electron state in the continuum. Because the electron Hamiltonian does not operate on the electron spins, the triplet excited $\text{Ne}^*[(3s); {}^3P_{0,2}]$ and $\text{Ne}^{**}[(3p); {}^3D_3]$ states are not coupled directly to the $\text{Ne}(^1S_0)$ ground state, so that the radiative mechanism is forbidden. In the *exchange* mechanism an electron of the target atom is transferred to the $(2p)^{-1}$ hole of the neon atom, with a simultaneous transition of the excited valence electron to a free-electron state. In a one-electron approximation the first electronic transition, e.g., $\text{Ar}(3p) \rightarrow \text{Ne}(2p)^{-1}$ for an argon target, is thought to determine the ionization rate, while the ejected $\text{Ne}(3s)$ [or $\text{Ne}(3p)$] valence electron has only a spectator role. In this commonly used approximation the autoionization width $\Gamma(R)$ is proportional to the squared overlap integral of the spatial wave functions of the two orbitals involved, as given by

TABLE I. The relative populations $c_{\sigma'}$ of the $(2p)^{-1}$ core hole for the atomic $\text{Ne}^{**}(\alpha_i; J; \Omega)$ states.

	$\Omega=0$	$\Omega=1$	$\Omega=2$	$\Omega=3$
$\text{Ne}^{**}[(3p); J=3]$	9/15	8/15	5/15	0
$\text{Ne}^*[(3s); J=2]$	2/3	1/2	0	
$\text{Ne}^*[(3s); J=0]$	1/3			

$$\Gamma(R) \sim \left| \int d\mathbf{r} [\Psi_{2p}^{\text{Ne}}(\mathbf{r})]^* \Psi_{3p}^{\text{Ar}}(\mathbf{r}) \right|^2 . \quad (4)$$

This approach results in two basic autoionization functions $\Gamma_{\sigma'}(R)$ and $\Gamma_{\pi'}(R)$, corresponding to the basic orientations of the $\text{Ne}(2p)^{-1}$ hole. The summation over all available $\text{Ar}(3p)$ states automatically selects the correct $\text{Ar}(3p)$ valence electron. Because the molecular $\text{Ne}^{**}(\alpha_i; J, \Omega)\text{-Ar}$ systems are not pure σ' or π' states, the autoionization widths are linear combinations of these basis functions, as given by

$$\Gamma_{J\Omega}(R) = c_{\sigma'} \Gamma_{\sigma'}(R) + (1 - c_{\sigma'}) \Gamma_{\pi'}(R) \quad (5)$$

with $c_{\sigma'}$ the relative σ' population (Table I). As shown by Driessen *et al.*,²¹ the basis functions can be described by a single exponential function with the onset of saturation at small internuclear distances, in agreement with experimental evidence.^{16,17,31} Semiclassical model calculations for the $\text{Ne}^*[(3s); {}^3P_{0,2}]\text{-Ar}$ system by Driessen *et al.*,²¹ using the real potential of Gregor and Siska⁹ and the autoionization widths of Eq. (5), show a cross-section ratio $Q(J=0)/Q(J=2) = 1.12$ at $E = 100$ meV that is much smaller than the experimental value $Q(J=0)/Q(J=2) = 1.31$. For the $\text{Ne}^{**}[(3p); {}^3D_3]\text{-Ar}$ system, however, the energy dependence of the polarization effect can be described in good approximation with this simple one-electron model.²¹

A formal analysis of the process of ionization is given within the framework of the Feshbach formalism³² with the discrete fine-structure states (before ionization) and the continuum states (after ionization) as two separate subspaces of Hilbert space. The projection-operator formalism was originally adapted to collisional ionization by O'Malley³³ and subsequently refined by Bieniek.³⁴ Autoionization widths for the $\text{He}^*(2^3S)\text{-H}_2$ system have been calculated with this theory by Hickman, Isaacson, and Miller.³⁵ For the case of associative ionization Jones and Dahler³⁶ have worked out this theory to a high degree of sophistication, especially concerning the choice of the quantum numbers involved.

In this paper we will adopt the projection-operator formalism for the $\text{Ne}^{**}(\alpha_i)\text{-Ar}$ collisions. In Sec. II we deal with the choice of the bound and continuum states used in the calculation and give a brief summary of the results and notations of the projection-operator analysis of the ionization process, together with an explicit formula for the autoionization width. In Sec. III a two-electron approximation for $\Gamma(R)$ is presented. Both electrons that make a transition in the ionization process are then taken into account. In Sec. IV we will discuss the aspects that have not yet been incorporated in the calculated ioniza-

tion widths for Ne^{*(*)}-Ar. Section V is devoted to semiclassical model calculations for the Ne^{*(*)}-Ar system with the basic autoionization width obtained in Sec. III. The semiclassical results are compared to available experimental data. In Sec. VI we present some concluding remarks.

II. PROJECTION-OPERATOR ANALYSIS OF PENNING IONIZATION

An extensive description of the application of the projection-operator analysis has been given by Jones and Dahler³⁶ for the process of associative ionization. We follow their approach to derive the autoionization width for Penning ionization in the local approximation.

The state vector $|\Psi\rangle\rangle$ that describes the Ne^{*(*)}-Ar collision system is a solution of the Schrödinger equation

$$(H - E)|\Psi\rangle\rangle = (T_{\text{kin}} + H_{\text{el}} - E)|\Psi\rangle\rangle = 0, \quad (6)$$

with H the total Hamiltonian consisting of the kinetic-energy operator T_{kin} and the electronic Hamiltonian H_{el} . We assume that H_{el} represents an electrostatic interaction and does not operate on the spin states of the electrons. The electron spins are therefore conserved quantities. Following the notation of Jones and Dahler³⁶ the double ket $|\Psi\rangle\rangle$ is the total state, describing both nuclei and electrons. We divide the total Hilbert space of electrons and nuclei in two subspaces: a Q subspace containing all "closed" channels (e.g., the initial Ne^{**}-Ar state with all electrons in a bound state) and a P subspace containing all "open" channels (e.g., the final Ne-Ar⁺ state with an unbound electron), with P and Q the corresponding projection operators.

We want to derive the effective Schrödinger equation for the projection $Q|\Psi\rangle\rangle$ onto the subspace of "closed"

channels. Using the properties of the operators P and Q we find

$$(\mathcal{H}_{QQ} - E)Q|\Psi\rangle\rangle = 0, \quad (7)$$

with the effective Hamiltonian \mathcal{H}_{QQ} given by

$$\mathcal{H}_{QQ} = H_{QQ} + H_{QP}G_P^+H_{PQ}. \quad (8)$$

The term $H_{QQ} = QHQ$ describes the direct coupling between the closed channels, i.e., the process of intramultiplet mixing. The second term $H_{QP}G_P^+H_{PQ}$, with G_P^+ the Green's operator, describes the indirect coupling of the bound states via the "open" channels, which represents an intramultiplet mixing process that is *not* due to radial coupling at an avoided crossing in the adiabatic potential curves.²⁵

To obtain an expression for the autoionization width $\Gamma(R)$, we have to investigate the effective Schrödinger equation [Eq. (7)]. We make an expansion of $|\Psi\rangle\rangle$ in kets $|PM_P, \Omega i E\rangle\rangle$, with P and M_P the quantum numbers of the total angular momentum and its projection on the internuclear axis, Ω the magnetic quantum number of the total electronic angular momentum along the internuclear axis, and i representing the remaining quantum numbers. These eigenkets can be constructed from the basis states $|\Omega i \mathbf{R}\rangle\rangle$ of the Q subspace according to

$$|PM_P, \Omega i E\rangle\rangle = \int d\mathbf{R} \frac{F_{\Omega i}^{PM_P}(E, R)}{R} \left[\frac{2P+1}{4\pi} \right]^{1/2} \times [D_{M_P, \Omega}^P(\hat{\mathbf{R}})]^* |\Omega i \mathbf{R}\rangle\rangle, \quad (9)$$

with $F_{\Omega i}^{PM_P}(E, R)$ the radial amplitudes and $D_{M_P, \Omega}^P(\hat{\mathbf{R}})$ an element of a representation of the rotation group. By substituting Eq. (9) in Eq. (7) one obtains an integro-differential equation for the radial amplitude:

$$\left[-\frac{\hbar^2}{2\mu} \frac{d^2}{dR^2} + E_{\Omega i}(R) + \frac{\hbar^2}{2\mu} \frac{P(P+1) - \Omega^2}{R^2} - E + \frac{\hbar^2}{2\mu} \left\langle\left\langle \Omega i \mathbf{R} \left| \left[\frac{J_1^2}{\hbar^2 R^2} - \frac{d^2}{dR^2} - 2 \frac{d}{dR} \right] \right| \Omega i \mathbf{R} \right\rangle\rangle F_{\Omega i}^{PM_P}(E, R) \right. \\ \left. = - \int_0^\infty dR' RR' \int d\hat{\mathbf{R}} \int d\hat{\mathbf{R}}' \frac{2P+1}{4\pi} [D_{M_P, \Omega}^P(\hat{\mathbf{R}})]^* D_{M_P, \Omega}^P(\hat{\mathbf{R}}') \langle\langle \Omega i \mathbf{R} | QHPG_P^+PHQ | \Omega i \mathbf{R}' \rangle\rangle F_{\Omega i}^{PM_P}(E, R') \right]. \quad (10)$$

The right-hand side of Eq. (10) represents a nonlocal potential term in Q space due to the coupling with the P subspace. Because the kinetic-energy operator T_{kin} maps the Q subspace onto itself, the Hamiltonians that appear explicitly in the coupling operator $QHPG_P^+PHQ$ may be replaced by the electronic Hamiltonian H_{el} . The matrix element can thus be written as

$$\langle\langle \Omega i \mathbf{R} | QHPG_P^+PHQ | \Omega i \mathbf{R}' \rangle\rangle = \sum_f \sum_{f'} \int dq \int dq' [V(R; \Omega f q, i)]^* \langle\langle \Omega f q \mathbf{R} | G_P^+ | \Omega f' q' \mathbf{R}' \rangle\rangle V(R'; \Omega f' q', i), \quad (11)$$

wherein

$$V(R; \Omega f q, i) = \langle \Omega f q \mathbf{R} | H_{\text{el}} | \Omega i \mathbf{R} \rangle \\ = \int d\mathbf{r}_n \phi_{q\lambda\mu}(\mathbf{r}_1 | \mathbf{R}) \phi_{\Omega f i}(\mathbf{r}_n - 1 | \mathbf{R}) \\ \times H_{\text{el}} \phi_{\Omega i}(\mathbf{r}_n | \mathbf{R}). \quad (12)$$

The double kets $|\Omega f q \mathbf{R}\rangle\rangle$ are the eigenstates of H_{el} in the P subspace, with q the wave number of the unbound elec-

tron and f representing all other quantum numbers. The electronic matrix element $V(R; \Omega f q, i)$ represents the coupling of the initial state with the ionized state through the electronic Hamiltonian H_{el} , which is diagonal in R . Asymptotically the wave function $\phi_{\Omega i}$ corresponds with the initial Ne^{*(*)}-Ar system with the Ne atom in an excited state and the Ar atom in the ground state; the wave function $\phi_{\Omega f i}$ describes asymptotically the Ne-Ar⁺ system with the Ne atom in the ground state and the Ar⁺

atom in the ionized state $\text{Ar}^+[(3p)^{-1}; {}^2P_{1/2}, {}^2P_{3/2}]$. The function $\phi_{q\lambda\mu}$ represents the continuum state, the emitted electron departing with an orbital angular momentum characterized by the quantum numbers λ and μ . Because the electric field is not centrally symmetric, the orbital angular momentum μ of the unbound electron is not a conserved quantity, but

$$\Omega = \Omega_I + \mu \quad (13)$$

is conserved. The Ar^+ ion acts as the center for the wave function $\phi_{q\lambda\mu}$, while the Ne atom has only a perturbing role. The matrix element $V(R; \Omega f q, i)$ is thus basically a two-center integral involving n electrons, with $n = 28$ for the $\text{Ne}^{*(*)}$ -Ar system.

To calculate the coupling matrix element of Eq. (11) with its "nonlocal" character is hardly possible. In order to make the integro-differential equation solvable, one applies the "local approximation,"^{37,38} resulting in

$$\langle\langle \Omega f q \mathbf{R} | G_p^+ | \Omega f' q' \mathbf{R}' \rangle\rangle = -i\pi\delta_{ff'}\delta(q - q')\delta(\mathbf{R} - \mathbf{R}')\delta(\varepsilon_q - \varepsilon(R)), \quad (14)$$

with $\varepsilon_q = \hbar^2 q^2 / 2m_e$ the kinetic energy of the emitted electron and $\varepsilon(R) = E_{\Omega_i}(R) - E_{\Omega_f}(R)$ the vertical ionization energy at internuclear distance R . The right-hand side of Eq. (10) then reduces to the product of the radial amplitude and an imaginary-valued potential $(i/2)\Gamma_i(R)$, with the autoionization width given by

$$\begin{aligned} \Gamma_i(R) &= 2\pi \sum_f \int dq |V(R; \Omega f q, i)|^2 \delta(\varepsilon_q - \varepsilon(R)) \\ &= \frac{2\pi m_e}{\hbar^2 q(R)} \sum_f |V(R; \Omega f q, i)|^2, \end{aligned} \quad (15)$$

with the local wave number of the free electron given by $q^2(R) = 2m_e \varepsilon(R) / \hbar^2$. The validity of the local approximation has recently been discussed in detail by Haywood and Delos³⁹ and by Morgner.⁴⁰

We now assume that only two electrons are actively involved in the ionization process of Eqs. (1) and (2). The two-center n -electron integral $V(R; \Omega f q, i)$ of Eq. (12) can thus be replaced by a two-center two-electron integral

$$\begin{aligned} V(R; \Omega f q, i) &= \int dx_1 dx_2 \phi_{\Omega f q}(x_1, x_2) \\ &\quad \times \frac{e^2}{4\pi\epsilon_0 |\mathbf{r}_1 - \mathbf{r}_2|} \phi_{\Omega_i}(x_1, x_2). \end{aligned} \quad (16)$$

The wave functions $\phi(x_1, x_2)$ include the spin degrees of freedom as well. The electronic Hamiltonian, given by the Coulomb interaction, does not operate on the electron spins, which are conserved quantities in this two-electron approximation.

III. TWO-ELECTRON APPROXIMATION FOR $\Gamma(R)$

A. Basic two-center two-electron integrals

Because only two electrons make a transition in the ionization process of Eqs. (1) and (2), the autoionization width can be determined by calculating the two-center two-electron integrals of Eq. (16). The total (spin and spatial) wave functions $\phi_{\Omega f q}(x_1, x_2)$ and $\phi_{\Omega_i}(x_1, x_2)$ of the two electrons must be antisymmetric. The spatial parts $\psi(\mathbf{r}_1, \mathbf{r}_2)$ of the total wave functions $\phi(x_1, x_2)$ are given by

$$\begin{aligned} \psi_{\Omega_i}(\mathbf{r}_1, \mathbf{r}_2) &= \frac{1}{\sqrt{2}} [\psi_{3s/3p}^{\text{Ne}}(\mathbf{r}_1) \psi_{3p}^{\text{Ar}}(\mathbf{r}_2) \\ &\quad \mp \psi_{3s/3p}^{\text{Ne}}(\mathbf{r}_2) \psi_{3p}^{\text{Ar}}(\mathbf{r}_1)], \\ \psi_{\Omega f q}(\mathbf{r}_1, \mathbf{r}_2) &= \frac{1}{\sqrt{2}} [\psi_{q\lambda\mu}^{\text{Ar}}(\mathbf{r}_1) \psi_{2p}^{\text{Ne}}(\mathbf{r}_2) \\ &\quad \mp \psi_{q\lambda\mu}^{\text{Ar}}(\mathbf{r}_2) \psi_{2p}^{\text{Ne}}(\mathbf{r}_1)], \end{aligned} \quad (17)$$

where the $- (+)$ sign refers to a triplet (singlet) two-electron spin state. The notation $3s/3p$ indicates either the $3s$ orbital or the $3p$ orbital. Because the Coulomb interaction does not operate on the electron spins, the spin quantum numbers are conserved quantities. The total wave functions $\phi(x)$ in the two-electron integrals can thus be replaced by the spatial part $\psi(\mathbf{r})$ of the wave function. The transition-matrix element $V(R; \Omega f q, i)$ can thus be written as a linear combination of a radiation and an exchange term:

$$V(R; \Omega f q, i) = V^{\text{exch}}(R; \Omega f q, i) \mp V^{\text{rad}}(R; \Omega f q, i), \quad (18)$$

with

$$\begin{aligned} V^{\text{exch}}(R; \Omega f q, i) &= \delta_{m_s m_{s,v}} \delta_{m_{s,c} m_{s,\text{Ar}}} \int d\mathbf{r}_1 d\mathbf{r}_2 \psi_{q\lambda\mu}^{\text{Ar}}(\mathbf{r}_1) \psi_{2p}^{\text{Ne}}(\mathbf{r}_2) \frac{e^2}{4\pi\epsilon_0 |\mathbf{r}_1 - \mathbf{r}_2|} \psi_{3s/3p}^{\text{Ne}}(\mathbf{r}_1) \psi_{3p}^{\text{Ar}}(\mathbf{r}_2), \\ V^{\text{rad}}(R; \Omega f q, i) &= \delta_{m_s m_{s,\text{Ar}}} \delta_{m_{s,c} m_{s,v}} \int d\mathbf{r}_1 d\mathbf{r}_2 \psi_{q\lambda\mu}^{\text{Ar}}(\mathbf{r}_1) \psi_{2p}^{\text{Ne}}(\mathbf{r}_2) \frac{e^2}{4\pi\epsilon_0 |\mathbf{r}_1 - \mathbf{r}_2|} \psi_{3s/3p}^{\text{Ne}}(\mathbf{r}_2) \psi_{3p}^{\text{Ar}}(\mathbf{r}_1), \end{aligned} \quad (19)$$

$m_{s,c}$, $m_{s,v}$, $m_{s,\text{Ar}}$, and m_s being the spin quantum numbers of the $\text{Ne}(2p)$ core orbital that is filled in the ionization process, the $\text{Ne}(3s/3p)$ valence electron, the $\text{Ar}(3p)$ electron, and the emitted electron, respectively.

The spatial wave functions of the atomic orbitals in the two-center two-electron integrals are all available and the integrals can be calculated. For the $\text{Ar}(3p)$ orbital we use the atomic wave functions of Clementi⁴¹ and for the

$\text{Ne}(2p/3s/3p)$ orbitals of the $\text{Ne}^{*(*)}$ atom we use the Hartree-Fock atomic wave functions calculated by Haberland.⁴² The wave function $\psi_{q\lambda\mu}^{\text{Ar}}$ of the free electron is calculated by solving the Schrödinger equation with a spherically symmetric potential representing the Ar^+e^- interaction. The screened Coulomb interaction we use is given by Aymar, Feneuille, and Klapisch⁴³ and has been used by Kucal, Hennecart, and Masnou-Seeuws⁴⁴ to cal-

culate the Ar^{*(*)} states. In the "local approximation" the kinetic energy of the emitted electron is given by

$$\varepsilon(R) = \frac{\hbar^2 q^2(R)}{2m_e} = E_{\Omega_i}(R) - E_{\Omega_f}(R). \quad (20)$$

The Coulomb wave function is calculated for quantum numbers of the orbital angular momentum up to $\lambda=7$. In order to minimize the computational effort, this calculation is carried out for a single kinetic energy ε_0 , given by the asymptotic energy difference

$$\begin{aligned} \varepsilon_0 &= E(\text{Ne}^{*(*)}) - E(\text{Ar}^+(^2P_{3/2})) \\ &= \begin{cases} 0.86 \text{ eV} & \text{for Ne}^*[(3s); ^3P_2] \\ 2.79 \text{ eV} & \text{for Ne}^{**}[(3p); ^3D_3] \end{cases}. \end{aligned} \quad (21)$$

The atomic energy difference between the two fine-structure states Ar^{+(^2P_{1/2}, ^2P_{3/2})} is 0.177 eV; the R dependence of the potential energies $E_{\Omega_i}(R)$ and $E_{\Omega_f}(R)$ broadens the energy spectrum of the emitted electron by approximately 0.1 eV, as reported by Hotop and co-workers.^{7,11,12} The approximation of using a single kinetic

energy ε_0 is therefore fully acceptable.

The calculation of the two-center two-electron integrals $V^{\text{exch}}(R; \Omega f q, i)$ and $V^{\text{rad}}(R; \Omega f q, i)$ is performed using the Gaussian ATMOL program^{45,46} running on a CYBER 205 supercomputer. The computer code has been developed at the University of Manchester. The atomic wave functions $\psi(\mathbf{r})$ are expanded in a series of spherical Gaussian-type orbitals,

$$\psi_{lm}(r) = r^l Y_{lm}(\theta, \varphi) \sum_i c_i \exp(-\alpha_i r^2). \quad (22)$$

The coefficients c_i and α_i of the atomic wave functions are given in Table II. The α_i coefficients have been chosen at fixed values and the c_i coefficients have been determined in a least-squares analysis. The advantage of Gaussian basis functions in quantum chemistry arises from the fact that the product of two Gaussians centered at different origins A and B results in another Gaussian centered between A and B . The magnetic substates of the spherical Gaussian-type orbitals lead to a large number of basic two-center two-electron integrals that have to be calculated:

$$\begin{aligned} V^{\text{exch}}(R; q \lambda \mu m_{l,c} m_{l,v} m_{l,\text{Ar}}) &= \int d\mathbf{r}_1 d\mathbf{r}_2 \psi_{q\lambda\mu}^{\text{Ar}}(\mathbf{r}_1) \psi_{2p, m_{l,c}}^{\text{Ne}}(\mathbf{r}_2) \frac{e^2}{4\pi\epsilon_0 |\mathbf{r}_1 - \mathbf{r}_2|} \psi_{3s/3p, m_{l,v}}^{\text{Ne}}(\mathbf{r}_1) \psi_{3p, m_{l,\text{Ar}}}^{\text{Ar}}(\mathbf{r}_2), \\ V^{\text{rad}}(R; q \lambda \mu m_{l,c} m_{l,v} m_{l,\text{Ar}}) &= \int d\mathbf{r}_1 d\mathbf{r}_2 \psi_{q\lambda\mu}^{\text{Ar}}(\mathbf{r}_1) \psi_{2p, m_{l,c}}^{\text{Ne}}(\mathbf{r}_2) \frac{e^2}{4\pi\epsilon_0 |\mathbf{r}_1 - \mathbf{r}_2|} \psi_{3s/3p, m_{l,v}}^{\text{Ne}}(\mathbf{r}_2) \psi_{3p, m_{l,\text{Ar}}}^{\text{Ar}}(\mathbf{r}_1). \end{aligned} \quad (23)$$

In this expression the quantum numbers μ , $m_{l,c}$, $m_{l,v}$, and $m_{l,\text{Ar}}$ refer to the electron states involved in the ionization process. To construct atomic Ne^{*(*)} or Ar⁺ states, however, we will use the magnetic quantum number that represents the five residual core electrons, which is reversed in sign and corresponds to Ne(2p)⁻¹ $\equiv |1, -m_{l,c}\rangle$ and Ar(3p)⁻¹ $\equiv |1, -m_{l,\text{Ar}}\rangle$. We thus have to be very careful about the sign of the m quantum number.

Because the Coulomb interaction is at least axially symmetric, the conservation of the magnetic quantum number [Eq. (13)] leads to the relation

$$\mu + m_{l,c} = m_{l,v} + m_{l,\text{Ar}}. \quad (24)$$

For Ne*(3s) we get a maximum of five basic combinations (μ , $m_{l,c}$; $m_{l,v}=0$, $m_{l,\text{Ar}}$) for each quantum number λ , while for Ne^{**}(3p) we end up with an upper limit of 14 basic combinations. These combinations are given in Table III. The two-center two-electron integrals of Eq. (23) have been calculated for all these combinations. This

has been done up to $\lambda=4$ and for 15 internuclear distances from $R=3a_0$ to $R=12a_0$. The total computing time for all these combinations amounted to 4 h.

B. Fine-structure-resolved autoionization widths

The purpose of this subsection is to determine the autoionization widths from the previous basic two-center two-electron integrals. To keep the effort within reasonable bounds, we make the assumption that the molecular Ne^{*(*)}-Ar states are equal to the antisymmetrized products of atomic Ne^{*(*)} and Ar states. We then have to know the composition of the Ne^{*(*)} and Ar⁺ states in terms of the basic ψ_{lm} orbitals. The Ne^{*(*)} states of interest are pure triplet states: Ne^{*(^3P₀, ^3P₂)} and Ne^{**(^3D₃)}. These $|LSJ\rangle$ -states result from the Ne^{+(2p)⁵} core and a (3s/3p) valence electron. They are conveniently given as particle-hole states⁴⁷ relative to the Ne closed-shell configuration using the second-quantization formalism

$$\begin{aligned} |\psi_{J\Omega}^{\text{Ne}^{**}}\rangle &= |\text{Ne}(2p)^{-1}(3p); L S J \Omega\rangle \\ &= \sum_{M_L M_S} (L M_L S M_S | J \Omega) \sum_{m_{l,c} m_{l,v}} (1 - m_{l,c} \ 1 m_{l,v} | L M_L) \\ &\quad \times \sum_{m_{s,c} m_{s,v}} (\frac{1}{2} - m_{s,c} \ \frac{1}{2} m_{s,v} | S M_S) \bar{a}_{(2p)^{-1} - m_{l,c} - m_{s,c}} a_{(3p) m_{l,v} m_{s,v}}^\dagger |\psi_{00}^{\text{Ne}}\rangle, \end{aligned} \quad (25)$$

TABLE II. The Gaussian expansion coefficients c_i and α_i of Eq. (22) of the electron orbitals used in the calculation of the two-center two-electron integrals of Eq. (23). The electron coordinates in Eq. (22) are given in a_0 , resulting in $c_i = (a_0)^{-l-3/2}$ for $l=0$ and $l=1$ and $c_i = (a_0)^{-\lambda-3/2}$ for $\lambda=0, 1, 2, \dots$. The unit of α_i is $(a_0)^{-1}$. The α_i coefficients have been chosen at fixed values and the c_i coefficients have been determined in a least-squares analysis.

	Ne(2p)	Ne(3s)	Ne(3p)	Ar(3p)
c_1	-0.402	0.377	-0.186	-0.056
c_2	-0.796	-0.008	0.148	-0.165
c_3	1.225	-0.996	0.715	0.128
c_4	0.015	0.105	-0.631	0.087
c_5		0.650	-0.052	0.001
α_1	20	10	8	2
α_2	8	1.5	0.85	0.7
α_3	0.4	0.24	0.09	0.26
α_4	0.01	0.05	0.013	0.06
α_5		0.02	0.005	0.01
	Coulomb wave $\psi_{q\lambda\mu}$ for Ne*(3s); $\epsilon=0.86$ eV			
	$\lambda=0$	$\lambda=1$	$\lambda=2$	$\lambda=3$
c_1	0.710	10.099	4.808	0.0153
c_2	-3.089	1.229	2.627	0.0012
c_3	2.373	-0.690	0.705	0.0010
c_4	0.625	-0.192	0.183	0.0001
c_5	-2.260	-0.010	0.080	0.0012
c_6	2.729	0.156	0.024	-0.0017
c_7	-2.418	0.183	0.010	0.0010
c_8	3.955	-0.622	-0.029	-0.0004
c_9	-4.068	0.515	0.025	
c_{10}	1.347	-0.047	-0.002	
α_1	20	20	20	1
α_2	2	4	4	0.11
α_3	1	0.9	1	0.033
α_4	0.11	0.3	0.5	0.0156
α_5	0.033	0.1	0.2	0.0090
α_6	0.0156	0.07	0.09	0.0060
α_7	0.0090	0.02	0.04	0.0030
α_8	0.0060	0.009	0.01	0.0018
α_9	0.0040	0.007	0.008	
α_{10}	0.0022	0.003	0.004	
	Coulomb wave $\psi_{q\lambda\mu}$ for Ne**(3p); $\epsilon=2.79$ eV			
	$\lambda=0$	$\lambda=1$	$\lambda=2$	$\lambda=3$
c_1	1.426	15.500	3.209	0.83×10^{-2}
c_2	-2.499	0.944	1.274	-0.20×10^{-2}
c_3	2.100	-0.241	0.778	0.35×10^{-2}
c_4	-1.264	-0.759	-0.141	0.38×10^{-2}
c_5	2.576	0.004	0.034	-0.30×10^{-2}
c_6	-3.314	-0.070	-0.042	0.84×10^{-3}
c_7	-1.363	0.897	0.157	-0.69×10^{-3}
c_8	6.925	-0.912	-0.308	
c_9	-7.649	0.318	0.196	
c_{10}	3.063	-0.101	-0.022	
α_1	20	20	5	0.25
α_2	3.4	4	2.1	0.11
α_3	0.44	1	0.718	0.0625
α_4	0.25	0.5	0.206	0.0210
α_5	0.11	0.2	0.065	0.0130
α_6	0.062	0.05	0.0195	0.0070
α_7	0.021	0.03	0.0070	0.0025
α_8	0.013	0.02	0.0050	
α_9	0.007	0.008	0.0039	
α_{10}	0.004	0.004	0.0022	

TABLE III. Combinations $(\mu, m_{l,c}; m_{l,v}, m_{l,Ar})$ in the basic integrals of Eq. (23). The magnetic quantum number of the total orbital angular momentum $M_L = m_{l,v} - m_{l,c}$ of the $\text{Ne}^{*(*)}$ atom [Eq. (25)] is indicated as well. The notation $\alpha-\beta$ has been introduced to refer to the basic integrals of Eq. (23).

Integral notation	$(\mu, m_{l,c}; m_{l,v}, m_{l,Ar})$	M_L	λ
$\text{Ne}^*(3s)$			
<i>a</i>	(0,0;0,0)	0	0,1,2, . . .
<i>b</i>	(1,0;0,1)	0	1,2,3, . . .
<i>c</i>	(0, -1; 0, -1)	1	0,1,2, . . .
<i>d</i>	(1, -1; 0, 0)	1	1,2,3, . . .
<i>e</i>	(2, -1; 0, 1)	1	2,3,4, . . .
$\text{Ne}^{**}(3p)$			
<i>f</i>	(0,0;0,0)	0	0,1,2, . . .
<i>g</i>	(0,1;1,0)	0	0,1,2, . . .
<i>h</i>	(1, -1; -1, 1)	0	1,2,3, . . .
<i>i</i>	(1,0;0,1)	0	1,2,3, . . .
<i>j</i>	(1,1;1,1)	0	1,2,3, . . .
<i>k</i>	(0,0;1, -1)	1	0,1,2, . . .
<i>l</i>	(0, -1; 0, -1)	1	0,1,2, . . .
<i>m</i>	(1, -1; 0, 0)	1	1,2,3, . . .
<i>n</i>	(1,0;1,0)	1	1,2,3, . . .
<i>o</i>	(2, -1; 0, 1)	1	2,3,4, . . .
<i>p</i>	(2,0;1,1)	1	2,3,4, . . .
<i>q</i>	(1, -1; 1, -1)	2	1,2,3, . . .
<i>r</i>	(2, -1; 1, 0)	2	2,3,4, . . .
<i>s</i>	(3, -1; 1, 1)	2	3,4,5, . . .

with \bar{a} the ‘‘hole creation operator’’ defined by

$$\bar{a}_{(nl)^{-1-m_{l,c}-m_{s,c}}} = (-1)^{l-m_{l,c}} (-1)^{1/2-m_{s,c}} \times a_{(nl)m_{l,c}m_{s,c}}. \quad (26)$$

The hole quantum numbers $-m_{l,c}$ and $-m_{s,c}$ refer to the $\text{Ne}^+(2p)^5$ core and are opposite in sign in comparison with the m quantum numbers of the $\text{Ne}(2p)$ state, which will be filled in the ionization process. The phase factor and the reversal of magnetic quantum numbers ensure that \bar{a} has the same transformation properties as the particle creation operator a^\dagger with the same $-m_{l,c}$ and $-m_{s,c}$ subscripts. Note that the quantum numbers J and Ω in Eq. (25) play the role of the collective quantum number i used previously. A similar expression applies to $|\psi_{J\Omega}^{\text{Ne}^*}\rangle$.

The final ionized state results from the $\text{Ar}^+(3p)^5$ core and can be written as a linear combination of the $\text{Ar}(3p)^{-1}$ hole states. Because the quantum numbers $m_{l,Ar}$ and $m_{s,Ar}$ refer to the $\text{Ar}(3p)$ electron, which is removed in the ionization process, the $\text{Ar}(3p)^{-1}$ hole state is described by m quantum numbers, which are reversed in sign:

$$\begin{aligned} |\psi_{J\Omega}^{\text{Ar}^+}\rangle &= |\text{Ar}(3p)^{-1}; J'\Omega_J\rangle \\ &= \sum_{m_{l,Ar}} \sum_{m_{s,Ar}} (1 - m_{l,Ar} \frac{1}{2} - m_{s,Ar}) |J'\Omega_J\rangle \\ &\quad \times \bar{a}_{(3p)^{-1-m_{l,Ar}-m_{s,Ar}}} |\psi_{00}^{\text{Ar}}\rangle. \end{aligned} \quad (27)$$

Experimental polarization effects in ionizing collisions have been determined, i.e., ionization cross sections for $\text{Ne}^{*(*)}\text{-Ar}$ with the excited neon atoms in an asymptotically pure magnetic substate.^{11-14,19,48} State selection of the final state $\text{Ar}^+(^2P_{1/2}, ^2P_{3/2})$ has also been performed.¹¹⁻¹⁴ Therefore we construct autoionization widths $\Gamma_{J',J\Omega}(R)$ which resolve both initial magnetic substates $\text{Ne}^{*(*)}(J,\Omega)$ and final fine-structure states $\text{Ar}^+(J')$. Of course the evolution of $|J,M\rangle_g$ to $|J,\Omega\rangle_R$ has still to be taken into account before a direct comparison is possible. By substituting Eqs. (25) and (27) into Eq. (19) we can write each of the n -electron H_{e1} matrix elements as a linear combination of the basic two-center two-electron integrals of Eq. (23), which have been calculated. Using the second-quantization formalism it is easily shown that for a triplet state the radiative term $V^{\text{rad}}(R; \Omega f q, i)$ is equal to zero (see the Appendix). The final expression for the autoionization width $\Gamma_{J',J\Omega}(R)$ is given by (see the Appendix)

$$\Gamma_{J',J\Omega}(R) = \frac{2\pi m_e}{\hbar^2 q(R)} \sum_{\lambda} f_{J',J\Omega}(R; \lambda), \quad (28)$$

with

$$\begin{aligned} f_{J',J\Omega}(R; \lambda) &= \sum_{\Omega_I} \sum_{\mu, m_s} |V^{\text{exch}}(R; f=J'\Omega_I \lambda \mu m_s q, i=J\Omega)|^2. \end{aligned} \quad (29)$$

The collective quantum numbers i and f are now specified explicitly in this expression. The matrix element $V^{\text{exch}}(R; f=J'\Omega_I \lambda \mu m_s q, i=J\Omega)$ is given by Eq. (A5). This matrix element is a linear combination of the basic two-center two-electron integrals of Eq. (23), determined by the Clebsch-Gordan coefficients of Eqs. (25) and (27). The functions $f_{J',J\Omega}(R)$ can be expressed in the basic two-center two-electron integrals of Table III, denoted $\alpha-\beta$. In Table IV these functions are given. The functions $f_{J',J\Omega}(R; \lambda)$ are equal to those obtained by Bussert¹³ for $\text{Ne}^*(3s)$. The total autoionization width $\Gamma_{J\Omega}(R)$ is obtained by summation over the final fine-structure states of the Ar^+ ions:

$$\Gamma_{J\Omega}(R) = \frac{2\pi m_e}{\hbar^2 q(R)} \sum_{\lambda} f_{J\Omega}(R; \lambda), \quad (30)$$

with

$$f_{J\Omega}(R; \lambda) = \sum_{J'} f_{J',J\Omega}(R; \lambda). \quad (31)$$

The functions $f_{J\Omega}(R, \lambda)$ are presented in Table V. From this table we obtain

$$f_{00}(R) = \frac{1}{5} [f_{20}(R) + 2f_{21}(R) + 2f_{22}(R)], \quad (32)$$

which implies that the average autoionization widths for $\text{Ne}^*(^3P_2)$ and $\text{Ne}^*(^3P_0)$ are equal. This can also be seen in Fig. 1, where we have presented the calculated autoionization widths for the $\text{Ne}^*(3s)\text{-Ar}$ system. Thus, as already stated in Sec. I, there is no mathematical evidence for a difference in the spherically averaged autoionization width for the two $\text{Ne}^*[(3s); ^3P_{0,2}]$ fine-structure states.

TABLE IV. The functions $f_{J\Omega,J}(R)$ of Eqs. (28) and (29) expressed in the basic two-center two-electron integrals, denoted by $a-s$ according to Table III.

Ne*(3s)	Ar ⁺ (² P _{1/2} ;J'=1/2)	Ar ⁺ (² P _{3/2} ;J'=3/2)
³ P ₀ ;J=0,Ω=0	$\frac{1}{9}[(a+2c)^2+2(\ell+d)^2]$	$\frac{1}{9}[2(a-c)^2+(\ell-2d)^2+3\ell^2+6e^2]$
³ P ₂ ;J=2,Ω=0	$\frac{1}{9}[2(a-c)^2+(2\ell-d)^2]$	$\frac{1}{9}[(2a+c)^2+2(\ell+d)^2+6\ell^2+3e^2]$
³ P ₂ ;J=2,Ω=1	$\frac{1}{12}[2(a-c)^2+(2\ell-d)^2+d^2+2e^2]$	$\frac{1}{12}[(2a+c)^2+2(\ell+d)^2+6\ell^2+3c^2+2d^2+4e^2]$
³ P ₂ ;J=2,Ω=2	$\frac{1}{3}(d^2+2e^2)$	$\frac{1}{3}(3c^2+2d^2+e^2)$
Ne**(3p)	Ar ⁺ (² P _{1/2} ;J'=1/2)	
³ D ₃ ;J=3,Ω=0	$\frac{1}{30}[4(\ell-g+k-\ell)^2+2(k-2i+j+m-n)^2]$	
³ D ₃ ;J=3,Ω=1	$\frac{1}{45}[4(\ell-g+k-\ell)^2+2(k-2i+j+m-n)^2+2(m-n+q)^2+(2o-2\mu+\nu)^2]$	
³ D ₃ ;J=3,Ω=2	$\frac{1}{18}[2(m-n+q)^2+(2o-2\mu+\nu)^2+\nu^2+2\delta^2]$	
³ D ₃ ;J=3,Ω=3	$\frac{1}{3}(\nu^2+2\delta^2)$	
Ne**(3p)	Ar ⁺ (² P _{3/2} ;J'=3/2)	
³ D ₃ ;J=3,Ω=0	$\frac{1}{30}[2(2\ell-2g-k+\ell)^2+(k-2i+j-2m+2n)^2+3(k-2i+j)^2+6(o-\mu)^2]$	
³ D ₃ ;J=3,Ω=1	$\frac{1}{45}[2(2\ell-2g-k+\ell)^2+(k-2i+j-2m+2n)^2+(2m-2n-q)^2+2(o-\mu-\nu)^2+3(k-2i+j)^2+6(k-\ell)^2+6(o-\mu)^2+3\delta^2]$	
³ D ₃ ;J=3,Ω=2	$\frac{1}{18}[(2m-2n-q)^2+2(o-\mu-\nu)^2+2\nu^2+4\delta^2+6(k-\ell)^2+3q^2]$	
³ D ₃ ;J=3,Ω=3	$\frac{1}{3}(3q^2+2\nu^2+\delta^2)$	

C. $\Gamma_{J,\Omega}(R)$ for Ne*(3s)-Ar

Using the expressions obtained in Sec. III B, the autoionization widths have been calculated. For the Ne*[(3s);³P_J,Ω]-Ar systems only the first three λ values contribute significantly. The functions $f_{J,\Omega}(R;\lambda)$ become negligible for $\lambda \geq 3$. The total widths $\Gamma_{J\Omega}(R)$ of Eq. (30) are shown in Fig. 1. The numerical values for $\Gamma_{J\Omega}(R)$ are given in Table VI.

The polarization effect $\Gamma_{J\Omega}(R)/\Gamma_{00}(R)$ is shown in Fig. 2. For large internuclear distances ($R \geq 5a_0$) the polar-

ization effect is practically proportional to the relative populations $c_{\sigma'}$ of the σ' configuration of the Ne($2p$)⁻¹ hole, as given in Table I. For an internuclear distance $R = 3.5a_0$ the polarization effect is equal to unity. In the one-electron approximation of Driessen *et al.*²¹ the two basic autoionization widths $\Gamma_{\sigma'}^0(R)$ and $\Gamma_{\pi}^0(R)$ are also equal for $R = 3.5a_0$. This confirms the interpretation of the Ne*(3s)-Ar ionization process as a one-electron exchange process accompanied by the emission of a spectator electron.

We have determined the fine-structure-dependent au-

TABLE V. The functions $f_{J\Omega}(R)$ of the total autoionization width of Eq. (30) expressed in the basic integrals of Table III, denoted by $a-s$.

Ne*(3s)	
³ P ₀ ;J=0,Ω=0	$\frac{1}{3}(a^2+2\ell^2+2c^2+2d^2+2e^2)$
³ P ₂ ;J=2,Ω=0	$\frac{1}{3}(2a^2+4\ell^2+c^2+d^2+e^2)$
³ P ₂ ;J=2,Ω=1	$\frac{1}{2}(a^2+2\ell^2+c^2+d^2+e^2)$
³ P ₂ ;J=2,Ω=2	$(c^2+d^2+e^2)$
Ne**(3p)	
³ D ₃ ;J=3,Ω=0	$\frac{1}{5}[(\ell-g)^2+(k-2i+j)^2+(k-\ell)^2+(m-n)^2+(o-\mu)^2]$
³ D ₃ ;J=3,Ω=1	$\frac{1}{15}[4(\ell-g)^2+2(k-2i+j)^2+4(k-\ell)^2+4(m-n)^2+4(o-\mu)^2+q^2+\nu^2+\delta^2]$
³ D ₃ ;J=3,Ω=2	$\frac{1}{3}[(k-\ell)^2+(m-n)^2+(o-\mu)^2+q^2+\nu^2+\delta^2]$
³ D ₃ ;J=3,Ω=3	$(q^2+\nu^2+\delta^2)$

TABLE VI. The autoionization widths $\Gamma_{J\Omega}(R)$ for the Ne*($|J,\Omega\rangle_R$)-Ar system as obtained in the two-electron approximation of Sec. III. The widths are given in eV.

R (units of a_0)	Ne*(3P_0) $\Omega=0$	Ne*(3P_2) $\Omega=0$	Ne*(3P_2) $\Omega=1$	Ne*(3P_2) $\Omega=2$
3.0	1.66×10^0	1.20×10^0	1.43×10^0	2.12×10^0
3.5	7.84×10^{-1}	7.64×10^{-1}	7.74×10^{-1}	8.04×10^{-1}
4.0	4.36×10^{-2}	6.54×10^{-1}	5.45×10^{-1}	2.18×10^{-1}
4.5	1.69×10^{-1}	2.79×10^{-1}	2.24×10^{-1}	5.92×10^{-2}
5.0	6.59×10^{-2}	1.13×10^{-1}	8.95×10^{-2}	1.87×10^{-2}
5.5	2.62×10^{-2}	4.65×10^{-2}	3.63×10^{-2}	5.87×10^{-3}
6.0	9.04×10^{-3}	1.65×10^{-2}	1.28×10^{-2}	1.58×10^{-3}
6.5	2.49×10^{-3}	4.64×10^{-3}	3.56×10^{-3}	3.36×10^{-4}
7.0	5.59×10^{-4}	1.06×10^{-3}	8.07×10^{-4}	6.38×10^{-5}
7.5	2.10×10^{-4}	3.95×10^{-4}	3.02×10^{-4}	2.59×10^{-5}
8.0	1.92×10^{-4}	3.63×10^{-4}	2.77×10^{-4}	2.59×10^{-5}
9.0	1.03×10^{-4}	1.98×10^{-4}	1.50×10^{-4}	7.61×10^{-6}
10.0	2.20×10^{-5}	4.24×10^{-5}	3.22×10^{-5}	1.55×10^{-6}
11.0	2.71×10^{-6}	5.16×10^{-6}	3.94×10^{-6}	2.60×10^{-7}
12.0	2.87×10^{-7}	5.29×10^{-7}	4.08×10^{-7}	4.44×10^{-8}

toionization widths $\Gamma_{J',J\Omega}(R)$ of Eq. (28). The ratio

$$W_{J',J\Omega}(R) = \Gamma_{J',J\Omega}(R) / \Gamma_{J\Omega}(R) \quad (33)$$

gives the fraction of the ionized states ending up in an $\text{Ar}^+(^2P_{J'})$ state. This ratio is illustrated in Fig. 3 for $J' = \frac{1}{2}$. In this figure we see that the $\text{Ne}^*(^3P_0; \Omega=0)$ state has a strong preference to produce $\text{Ar}^+(^2P_{3/2})$ ions. Only about 10% of the produced Ar^+ ions end up in an $\text{Ar}^+(^2P_{1/2})$ state. For the $\text{Ne}^*(^3P_2; \Omega=0,1)$ states we observe no preference to produce a specific fine-structure state of the Ar^+ ion, while the $\text{Ne}^*(^3P_2; \Omega=2)$ state produces almost exclusively $\text{Ar}^+(^2P_{3/2})$ ions. From Table IV we can understand this feature. The functions $f_{J',J\Omega}(R)$ contain coherent sums of the integrals $a-e$.

The integrals b and d only give contributions for $\lambda \geq 1$, the integral e for $\lambda \geq 2$. Their absolute values are small compared to a :

$$|b/a| < 0.15, \quad |d/a| < 0.25, \quad |e/a| < 0.02. \quad (34)$$

The ratio c/a has an R dependence as shown in Fig. 4. It is practically independent of the quantum number λ . The average ratio is

$$c/a \approx -0.18 \quad (35)$$

in the range $R \geq 6a_0$ as relevant for a thermal collision energy $E \approx 60$ meV. Taking this ratio and neglecting the integrals b, d , and e , we obtain the ratios

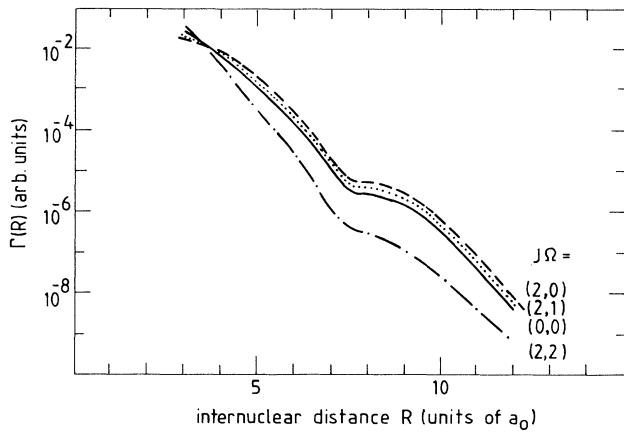


FIG. 1. The total autoionization widths $\Gamma_{J\Omega}(R)$ for the Ne*(3s)-Ar system. An exponential behavior is observed. The dip at $R = 7a_0$ is caused by the two-electron integrals a and c of Table III, which have a zero at $R = 7a_0$ for $\lambda=0$ and 2. These integrals have the largest contribution to the autoionization width.

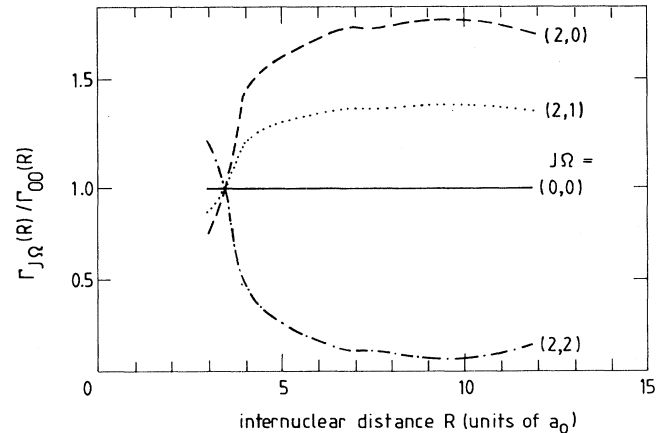


FIG. 2. The polarization effect $\Gamma_{J\Omega}(R)/\Gamma_{00}(R)$ for the Ne*[(3s)]-Ar system. Asymptotically this polarization effect is proportional to the relative populations of the σ' configuration of the $\text{Ne}(2p)^{-1}$ hole of Table I, resulting in $c_{\sigma'}(J\Omega)/c_{\sigma'}(00) = 2, 1.5$, and 0 for $(J,\Omega) = (2,0), (2,1)$, and $(2,2)$, respectively. The spherical average $\Gamma_2(R) = \frac{1}{5}[\Gamma_{20}(R) + 2\Gamma_{21}(R) + 2\Gamma_{22}(R)]$ is equal to $\Gamma_{00}(R)$.

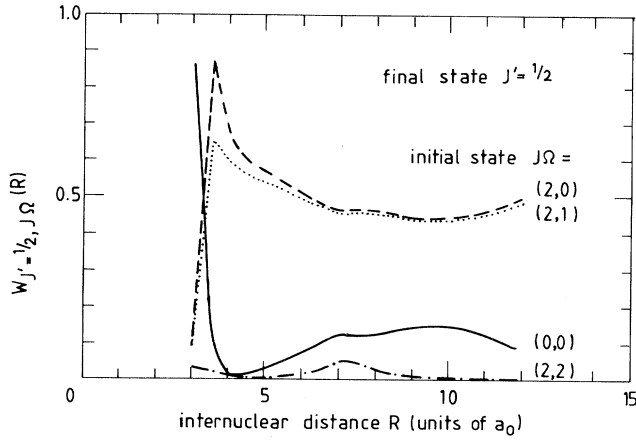


FIG. 3. The ratio of the fine-structure-dependent autoionization widths $W_{J', J\Omega}(R) = \Gamma_{J', J\Omega}(R) / \Gamma_{J\Omega}(R)$ for $J' = 1/2$, which represents the fraction of the produced Ar^+ ions ending up in an $\text{Ar}^+(^2P_{1/2})$ state. For $J' = 3/2$ the ratio is $W_{3/2, J\Omega}(R) = 1 - W_{1/2, J\Omega}(R)$.

$$\begin{aligned} f_{1/2,00}(R)/f_{3/2,00}(R) &= 0.15, \\ f_{1/2,20}(R)/f_{3/2,20}(R) &= f_{1/2,21}(R)/f_{3/2,21}(R) \\ &= 0.84, \\ f_{1/2,22}(R)/f_{3/2,22}(R) &= 0. \end{aligned} \quad (36)$$

For a direct and simple comparison with Morgner's²² analysis of experimental data we introduce the autoionization width for unpolarized projectiles as

$$\Gamma_{J', J} = \frac{1}{2J+1} \sum_{\Omega} g_{\Omega} \Gamma_{J', J\Omega} \quad (37)$$

with $g_0 = 1$ and $g_{\Omega} = 2$ for $\Omega \neq 0$. We then find

$$\begin{aligned} \Gamma_{3/2,0}/\Gamma_{1/2,0} &= 6.7, \\ \Gamma_{3/2,2}/\Gamma_{1/2,2} &= 1.3. \end{aligned} \quad (38)$$

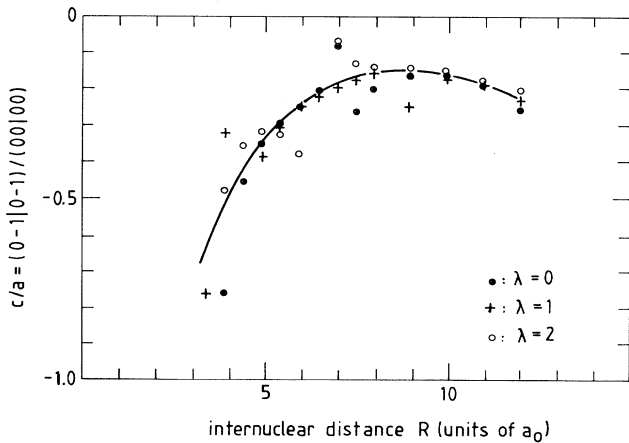


FIG. 4. The R dependence of the ratio c/a of the two-center two-electron integrals, denoted c and a according to Table III, for $\lambda = 0, 1$, and 2 . This ratio is practically independent of the quantum number λ of the emitted electron.

Based on the experimental results of Hotop, Lorentzen, and Zastrow⁷ for state selection of the final fine-structure $\text{Ar}^+(^2P_{1/2}, ^2P_{3/2})$ states at a collision energy of $E = 60$ meV, Morgner²² has estimated the ratios of the two-center two-electron integrals for the $\text{Ne}^*(3s)\text{-Ar}$ system. As in our analysis, the initial state is assumed to be a pure atomic state [Eq. (25)]. The two-center integrals $a-e$ serve as parameters for the autoionization widths $\Gamma_{J', J\Omega}(R)$, which thus demonstrate an R -independent relative scaling according to the functions $f_{J', J\Omega}(R)$ (see Table IV). The experimental data on $\text{Ne}^*(^3P_0, ^3P_2)$ are obtained with unpolarized projectiles. Therefore the relevant cross sections are assumed to be proportional to

$$Q(J'; J) \sim \Gamma_{J', J}. \quad (39)$$

The parameters are determined from the experimental fine-structure branching ratios⁷ for $E = 60$ meV,

$$\begin{aligned} {}^0B &= Q(3/2; 0)/Q(1/2; 0) = 3.94(14), \\ {}^2B &= Q(3/2; 2)/Q(1/2; 2) = 1.51(7). \end{aligned} \quad (40)$$

From this analysis Morgner finds that the integrals $a-e$ should satisfy the conditions

$$\begin{aligned} \frac{c}{a} &= -0.106, \\ |c| &< |c|, \quad |d| < |c|, \quad |e| < |c|. \end{aligned} \quad (41)$$

When comparing the *ab initio* and experimental values for the ratio c/a , as given in Eqs. (35) and (41), we have to consider the sensitivity of c/a for errors in the fine-structure branching ratios ${}^J B$ of Eq. (40). Assuming $b=d=e=0$ we can directly derive

$$\frac{\Delta(c/a)}{c/a} = 1.4 \frac{\Delta({}^0B)}{{}^0B} - 4.0 \frac{\Delta({}^2B)}{{}^2B}, \quad (42)$$

which relates the relative variation of c/a to the error in either 0B or 2B . Of course, each of the parameters 0B or 2B is sufficient to determine the value of c/a . The experimental errors [Eq. (40)] are $\Delta({}^0B)/{}^0B = 3.5\%$ and $\Delta({}^2B)/{}^2B = 4.6\%$, leading to $\Delta(c/a)/(c/a) \approx 5\%$ when using 0B or 20% when using 2B and thus

$$\begin{aligned} c/a &= -0.106 \pm 0.005 \quad \text{for } {}^0B, \\ c/a &= -0.106 \pm 0.02 \quad \text{for } {}^2B. \end{aligned} \quad (43)$$

However, the assumption in Eq. (39) of a linear relation between cross section and autoionization width introduces an extra systematic error in this simple analysis. Due to saturation effects in the cross section, the actual ratio $\Gamma_{3/2,0}/\Gamma_{1/2,0}$ will be larger than the experimental fine-structure branching ratio 0B . This effect can be of the order of $+5\%$ to $+10\%$, resulting in an extra error $\Delta(c/a)/(c/a) \approx +8\%$ to $+14\%$ for the value based on the experimental result of 0B . Taking into account this sensitivity we can conclude that our *ab initio* value for

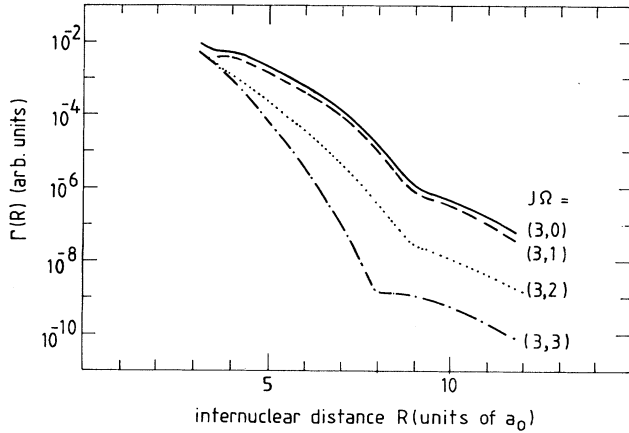


FIG. 5. The total autoionization widths $\Gamma_{J\Omega}(R)$ for the $\text{Ne}^{**}(3p)\text{-Ar}$ system. An exponential behavior is observed and the onset of saturation is clearly observed for the $\text{Ne}^{**}(^3D_3; \Omega=0,1)\text{-Ar}$ systems at $R \approx 4a_0$. For large internuclear distances the ratio $\Gamma_{30}(R)/\Gamma_{33}(R)$ is very large, almost three orders of magnitude.

c/a is, although slightly too large, in fair agreement with the value derived by Morgner²² from Hotop's experimental results.

In Sec. VC we will present semiclassical calculations with the calculated autoionization widths $\Gamma_{J',J\Omega}(R)$. An important conclusion can already be made at this stage. The average value of the $\Gamma_{2\Omega}$ widths for $\text{Ne}^*(^3P_2)$ is equal to Γ_{00} for $\text{Ne}^*(^3P_0)$, which does not give a new point of view to explain the $Q(^3P_0)/Q(^3P_2)$ ratio beyond the analysis given by Driessen *et al.*²¹ in terms of the two-state basis $\Gamma_{\sigma'}$ and $\Gamma_{\pi'}$. In Sec. IV we will discuss this discrepancy in more detail.

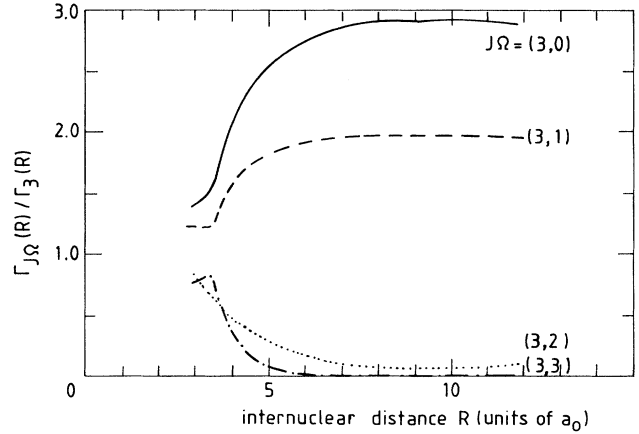


FIG. 6. The polarization effect $\Gamma_{3\Omega}(R)/\Gamma_3(R)$ for the $\text{Ne}^{**}(^3D_3)\text{-Ar}$ system. The $\text{Ne}^{**}(^3D_3; \Omega=0,1)\text{-Ar}$ systems ionize very well, whereas the $\text{Ne}^{**}(^3D_3; \Omega=2,3)\text{-Ar}$ systems ionize very poorly.

D. $\Gamma_{J',J\Omega}(R)$ for $\text{Ne}^{**}(3p)\text{-Ar}$

The expressions for $\Gamma_{J',J\Omega}(R)$ and $\Gamma_{J\Omega}(R)$ of Eqs. (28) and (30) have been used to calculate the autoionization widths for the $\text{Ne}^{**}(^3D_3, \Omega)\text{-Ar}$ system. The average autoionization width $\Gamma_3(R)$ for $\text{Ne}^{**}(^3D_3)\text{-Ar}$ is given by

$$\Gamma_3(R) = \frac{1}{7} [\Gamma_{30}(R) + 2\Gamma_{31}(R) + 2\Gamma_{32}(R) + 2\Gamma_{33}(R)]. \quad (44)$$

The calculated widths $\Gamma_{3\Omega}(R)$ are presented in Fig. 5. Numerical values for $\Gamma_{3\Omega}(R)$ are given in Table VII. The polarization effects $\Gamma_{3\Omega}(R)/\Gamma_3(R)$ are given in Fig. 6. For large internuclear distances ($R > 5a_0$) the polarization effect is very pronounced. It is, however, not proportional to the relative populations $c_{\sigma'}$ of the σ' configuration of the $\text{Ne}(2p)^{-1}$ hole for the atomic Ne^{**} states as given in Table I. The construction of the autoionization widths in the one-electron approximation is

TABLE VII. The autoionization widths $\Gamma_{J\Omega}(R)$ for the $\text{Ne}^{**}(^3D_3; |J, \Omega\rangle_{\text{R}})\text{-Ar}$ system as obtained in the two-electron approximation of Sec. III. The widths are given in eV.

R (units of a_0)	$\text{Ne}^*(^3D_3)$ $\Omega=0$	$\text{Ne}^*(^3D_3)$ $\Omega=1$	$\text{Ne}^*(^3D_3)$ $\Omega=2$	$\text{Ne}^*(^3D_3)$ $\Omega=3$
3.0	1.92×10^{-1}	1.67×10^{-1}	1.14×10^{-1}	1.03×10^{-1}
3.5	8.40×10^{-2}	6.77×10^{-2}	3.71×10^{-2}	4.64×10^{-2}
4.0	8.13×10^{-2}	6.08×10^{-2}	1.91×10^{-2}	1.60×10^{-2}
4.5	5.70×10^{-2}	4.14×10^{-2}	9.29×10^{-3}	4.56×10^{-3}
5.0	3.13×10^{-2}	2.23×10^{-2}	3.79×10^{-3}	1.14×10^{-3}
5.5	1.65×10^{-2}	1.15×10^{-2}	1.46×10^{-3}	2.61×10^{-4}
6.0	8.86×10^{-3}	6.13×10^{-3}	5.73×10^{-4}	5.61×10^{-5}
6.5	4.58×10^{-3}	3.14×10^{-3}	2.18×10^{-4}	1.10×10^{-5}
7.0	2.09×10^{-3}	1.42×10^{-3}	7.51×10^{-5}	1.83×10^{-6}
7.5	7.83×10^{-4}	5.31×10^{-4}	2.22×10^{-5}	2.20×10^{-7}
8.0	2.32×10^{-4}	1.57×10^{-4}	5.50×10^{-6}	2.11×10^{-8}
9.0	1.69×10^{-5}	1.15×10^{-5}	4.24×10^{-7}	1.95×10^{-8}
10.0	8.01×10^{-6}	5.41×10^{-6}	1.83×10^{-7}	9.53×10^{-9}
11.0	2.68×10^{-6}	1.81×10^{-6}	7.01×10^{-8}	3.22×10^{-9}
12.0	6.63×10^{-7}	4.52×10^{-7}	2.46×10^{-8}	1.04×10^{-9}

therefore not correct. In contrast, for $R = 3.5a_0$ the polarization effect tends to become unity, which is in agreement with the two-state basis $\Gamma_{\sigma}^0(R)$ and $\Gamma_{\pi}^0(R)$ of Driessen *et al.*,²¹ indicating that the overlap integral of Eq. (4) is the dominant factor in the calculated two-center two-electron integrals of Eq. (23).

The ratio $W_{J',J\Omega}(R)$ of the fine-structure-dependent autoionization widths $\Gamma_{J',J\Omega}(R)$ of Eq. (33) is shown in Fig. 7 for $J' = \frac{1}{2}$. From this figure we see that the $\text{Ne}^{**}(^3D_3; \Omega=0,1)$ states have no preference to produce a specific fine-structure state of the Ar^+ ion. The $\text{Ne}^{**}(^3D_3; \Omega=2)$ state produces approximately 85% of the Ar^+ ions in the $\text{Ar}^+(^2P_{3/2})$ state and about 15% in an $\text{Ar}^+(^2P_{1/2})$ state. For the $\text{Ne}^{**}(^3D_3; \Omega=3)$ states we observe almost exclusively $\text{Ar}^+(^2P_{3/2})$ ions. The two-center two-electron integrals of Table III that contribute most significantly are ℓ and ℓ , which represent the same $(\mu, m_{l,c}; m_{l,v}, m_{l,\text{Ar}})$ combinations that are dominant for Ne^*-Ar (ℓ corresponding to a and ℓ corresponding to c). The R dependence of the ratio ℓ/ℓ is shown in Fig. 8. It is practically equal to the ratio c/a of Fig. 4. The absolute values of the other two-electron integrals compared to ℓ are

$$\begin{aligned} |g/\ell|, |m/\ell|, |n/\ell| &< 0.25, \\ |j/\ell|, |q/\ell| &< 0.10, \\ |i/\ell|, |k/\ell| &< 0.05, \\ |h/\ell|, |o/\ell|, |r/\ell|, |s/\ell| &\approx 0.0. \end{aligned} \quad (45)$$

For all $\text{Ne}^{**}[(2p)^5(3p); J=1,2,3]-\text{Ar}$ systems ionization cross sections have been measured by Bussert *et al.*,^{12,13} resolving the fine-structure states of the produced Ar^+ ion. For $\text{Ne}^{**}(^3D_3)-\text{Ar}$ the fine-structure branching ratio at $E = 110$ meV is

$${}^3B = Q(3/2; 3)/Q(1/2; 3) \approx 1.60(3). \quad (46)$$

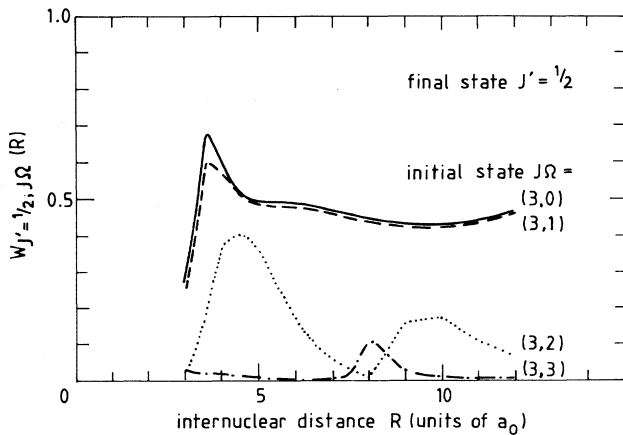


FIG. 7. The ratio $W_{J',J\Omega}(R)$ for $J' = 1/2$ of the fine-structure-dependent autoionization widths for the $\text{Ne}^{**}(^3D_3)-\text{Ar}$ system. The ratio $W_{J',J\Omega}(R) = \Gamma_{J',J\Omega}(R)/\Gamma_{J\Omega}(R)$ represents the fraction of the produced Ar^+ ions ending up in $\text{Ar}^+(^2P_{J'})$ state.

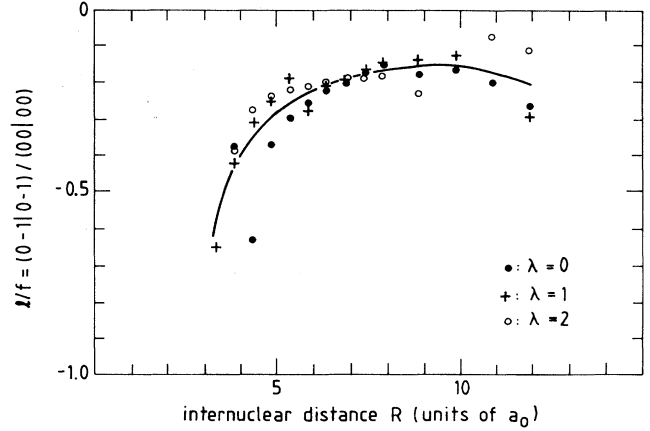


FIG. 8. The R dependence of the ratio ℓ/ℓ of the two-center two-electron integrals, denoted ℓ and ℓ according to Table III. This ratio is practically independent of the quantum number λ of the emitted electron. We observe the same behavior as the ratio c/a of Fig. 9. According to Table III these integrals represent the same $(\mu, m_{l,c}; m_{l,v}, m_{l,\text{Ar}})$ combinations ($a \equiv \ell$ and $c \equiv \ell$).

The ratios of the two-center two-electron integrals for the $\text{Ne}^{**}(3p)-\text{Ar}$ system have been estimated by Bussert as well. Similar to Morgner's analysis,²² which has been described briefly in Sec. III C, the integrals serve as parameters for the autoionization widths $\Gamma_{J',J\Omega}(R)$. In his analysis Bussert takes into account only those two-electron integrals in which the magnetic quantum numbers of the individual electrons are conserved, i.e., $\mu = m_{l,v}$ and $m_{l,c} = m_{l,\text{Ar}}$ (ℓ, ℓ, j, n , and q). In a least-squares analysis of the cross-section data according to Eq. (39), the integral ratios were fixed at

$$\begin{aligned} n/\ell &= 0.71 \pm 0.11, \quad \ell/\ell = 0.04 \pm 0.08, \\ j/\ell &= -0.14 \pm 0.03, \quad q/\ell = -0.18 \pm 0.09. \end{aligned} \quad (47)$$

The uncertainties in these ratios are very large. In comparison with our *ab initio* results, we conclude that it is not justifiable to neglect the integrals g and m . Moreover, in comparison to the $\text{Ne}^*(3s)-\text{Ar}$ case, the assumption of R -independent ratios of overlap integrals is less justified because a much larger range $R \geq 4.5a_0$ contributes. This is due to the steeper repulsive branch at smaller internuclear distances and the deeper potential well, which both result in smaller values of the classical turning point at the same energy and impact parameter. Therefore it is no surprise that the integral ratios are not in agreement with our integral ratios.

In Sec. V B we will present semiclassical calculations for the $\text{Ne}^{**}(^3D_3)-\text{Ar}$ systems. The pronounced polarization effect in $\Gamma_{3\Omega}(R)/\Gamma_3(R)$ should be able to explain the experimental polarized-atom cross sections, measured for $\text{Ne}^{**}(^3D_3)-\text{Ar}$ by Driessen *et al.*²¹ "Locking" phenomena will be included in order to obtain the correct energy dependence of the polarized-atom cross sections as discussed by Driessen *et al.*²¹

IV. DISCUSSION OF $\Gamma_{J',J\Omega}(R)$ FOR Ne*(3s)-Ar

The autoionization widths we obtained in Secs. III C and III D show a pronounced Ω splitting. The experimental polarization effects observed in the ionization cross section $^J Q^{|M|}(E)$ for an asymptotic Ne*(*)($|J, M\rangle_g$) state colliding with Ar can thus be explained as will be shown in the next section. For the Ne*(3s)-Ar system the average autoionization widths for 3P_2 and 3P_0 were found to be equal in our model [Eq. (32)]. As stated earlier in Sec. III C this means that the ratio $Q(^3P_0)/Q(^3P_2)$ cannot be explained by our present attempt to go beyond the analysis given by Driessen *et al.*²¹ in terms of the two-state basis $\Gamma_{\sigma'}(R)$ and $\Gamma_{\pi}(R)$.

In our analysis we assumed the molecular states Ne*($|J, \Omega\rangle_R$)-Ar to be pure atomic states [Eq. (25)]. The replacement of a pure state by a linear combination complicates the formulas. Bussert¹³ has calculated the adiabatic eigenstates for Ne*(*)-Ar for $R = 5.5a_0$ and $10a_0$. For $R = 5.5a_0$ the Ne*($^3P_0, ^3P_2$) states are still 97% atomic states, which indicates that the above assumption is legitimate.

Only the exchange term has been taken into account in the autoionization widths $\Gamma_{J',J\Omega}(R)$ [Eqs. (29)–(31)]. The calculation of the two-center two-electron integrals of Eq. (23) showed that the radiation mechanism and the exchange mechanism are competitive for small internuclear distances ($R < 6a_0$). For larger internuclear distances the radiative term is dominant, because it decreases asymptotically as R^{-6} while the exchange term decreases exponentially. The admixing of a very small fraction of the Ne*(1P_1) singlet state for large R values might possibly increase the autoionization width for Ne*(3P_0)-Ar more than for Ne*(3P_2)-Ar. The molecular adiabatic eigenstates for Ne*-Ar can be determined by diagonalizing the total Hamiltonian in the $|LSJ\Omega\rangle$ representation. For $\Omega=0$ the constraint of reflection symmetry generates distinct + and – classes, containing the odd and even J states, respectively. Therefore the Ne*($^3P_0, ^3P_2; \Omega=0$) states cannot admix the Ne*($^1P_1; \Omega=0$) state. Only for the Ne*($^3P_2; \Omega=1$)-Ar system can a singlet contribution be obtained. This implies that only the autoionization width for the Ne*($^3P_2; \Omega=1$)-Ar system can be increased, leaving us with an unexplained $Q(^3P_0)/Q(^3P_2)$ ratio. However, the results of Bussert¹³ for the adiabatic eigenstates in terms of atomic $|LSJ\Omega\rangle$ states show that the admixing is negligible at these large distances and no influence at all is to be expected from the radiative mechanism.

For smaller internuclear distances ($R < 5.5a_0$), the mixing of $|LSJ\Omega\rangle$ states is no longer negligible. If the exchange and radiative terms, which are of comparable size now, were to interfere destructively for the singlet state according to Eq. (33), the autoionization width for Ne*($^3P_2; \Omega=1$)-Ar may be diminished. The small mixing of Ne*($^3P_0, ^3P_2; \Omega=0$) states may even result in an increase of the ionization rate for 3P_0 at the expense of 3P_2 . Because $\Gamma_{J',J\Omega}(R)$ contains coherent terms, this increase can be more than proportional to the admixed population. We have to realize, however, that the range of impact parameters that probes these small internuclear dis-

tances is very limited (if existing at all at thermal energy), which would still result in a rather small effect on the total cross section.

This leaves us with an unexplained cross-section ratio $Q(^3P_0)/Q(^3P_2)$. The only approach that remains is a full analysis with molecular states, which is beyond the scope of this paper. In view of the above discussion it is not clear whether this will solve this problem.

One might be tempted to ascribe the discrepancy of our theoretical result with the experimental ratio $Q(^3P_0)/Q(^3P_2)$ to the fact that we left out (anti) symmetrization of the Q basis states $|\Omega; iR\rangle$ with respect to a plane through the internuclear axis. Note, however, that it is not necessary to introduce reflection parity from the beginning: it is included automatically if one includes the coupling of the z' magnetic quantum number by the J_z^2 operator in Eq. (10). If instead reflection parity had been included from the beginning via a superposition of opposite z' magnetic quantum numbers, this would not have changed the autoionization widths $\Gamma(R)$: the operator $QHPG_p^+PHQ$ is axially symmetric and reflection invariant and is therefore diagonal in Ω with diagonal elements independent of the sign of Ω .

V. SEMICLASSICAL CALCULATIONS

A. Semiclassical model

To calculate the polarized-atom cross sections $^J Q^{|M|}(E)$ from the Ω -dependent optical potentials [Eq. (3)], we use the semiclassical model as described by Driessen *et al.*^{20,21} Basically this model is a classical trajectory calculation of an asymptotic pure magnetic substate Ne*(*)($|J, M\rangle_g$) colliding with an Ar atom with impact parameter b .

Rotational coupling describes the scrambling of the Ω distribution caused by the rotation of the internuclear axis. The rotational coupling is effective if the Ω splitting in the real potential $V_\Omega(R)$ is negligible. In this situation the Ω quantum number is not a conserved quantity and a space-fixed description of the \mathbf{J} vector is applicable. For a large Ω splitting in the real potentials $V_\Omega(R)$ a torque operates on the total electronic angular momentum \mathbf{J} . The Ω splitting is characterized by

$$\Delta V^{\max}(R) = \max[V_\Omega(R) - V_{\Omega'}(R)], \quad (48)$$

and can thus be translated into a precession frequency $\omega_{\text{prec}}(R)$ of the \mathbf{J} vector about the internuclear axis, as given by

$$\omega_{\text{prec}}(R) = \Delta V^{\max}(R) / (J\hbar). \quad (49)$$

This precession frequency $\omega_{\text{prec}}(R)$ has to be compared to the angular velocity $\dot{\phi}(R)$ of the rotating internuclear axis. The space-fixed description of the electronic angular momentum \mathbf{J} is valid in the situation that $\dot{\phi}(R) \gg \omega_{\text{prec}}(R)$. On the other hand, if $\dot{\phi}(R) \ll \omega_{\text{prec}}(R)$ a body-fixed description of \mathbf{J} is necessary. There is a gradual transition between the two descriptions. In our semiclassical model, however, we introduce a sharp boundary at R_L between the regions where the two \mathbf{J}

descriptions are applicable. This locking radius R_L can be calculated with the condition

$$\omega_{\text{prec}}(R_L) = f_L \dot{\phi}(R_L), \quad (50)$$

where f_L is a locking factor. Previous calculations of Manders *et al.*²⁵ for the Ne^{**}-He intramultiplet mixing process and of Driessen *et al.*^{20,21} for the Ne^{**}-Ar ionization process indicate this locking factor to be $f_L = 4$. Especially the energy dependence of the polarization effect in the ionization cross section depends critically on this locking factor.

In the space-fixed description of the electronic angular momentum \mathbf{J} , we assume that the Ω distribution of the local molecular states $\sum_{\Omega} c_{\Omega}(\mathbf{R})|J, \Omega\rangle$ moves along a single trajectory, which is calculated with an average real potential $V(R)$ given by

$$V(\mathbf{R}) = \frac{\sum_{\Omega=-J}^{+J} [c_{\Omega}(\mathbf{R})]^2 V_{\Omega}(R)}{\sum_{\Omega=-J}^{+J} [c_{\Omega}(\mathbf{R})]^2} \quad (51)$$

with $c_{\Omega}(\mathbf{R})$ the R -dependent coefficients of the molecular state $\sum_{\Omega} c_{\Omega}(\mathbf{R})|J, \Omega\rangle$. The potential is normalized by the total population $\sum_{\Omega} [c_{\Omega}(\mathbf{R})]^2$, which is less than or equal to unity, because a fraction of the $|J, \Omega\rangle$ states is lost in the ionization process. The evolution of the local molecular Ω distribution $c_{\Omega}(\mathbf{R})$ to a new distribution $c_{\Omega}(\mathbf{R} + \Delta\mathbf{R})$ is given by

$$c_{\Omega}(\mathbf{R} + \Delta\mathbf{R}) = \sum_{\Omega'=-J}^{+J} d_{\Omega\Omega'}^J(\Delta\phi) c_{\Omega'}(\mathbf{R}) \quad (52)$$

with $d_{\Omega\Omega'}^J(\Delta\phi)$ the Wigner d function and $\Delta\phi$ the angle in the collision plane between the two orientations of $\phi(\mathbf{R})$ and $\phi(\mathbf{R} + \Delta\mathbf{R})$ of the internuclear axis.

When the body-fixed description is appropriate, the Ω splitting in the real potential $V_{\Omega}(R)$ is not negligible. In our semiclassical model, each local molecular state $|J, \Omega\rangle$ then follows a unique trajectory determined only by $V_{\Omega}(R)$ and no Ω mixing due to rotational coupling occurs. Therefore the particle trajectory splits in $J + 1$ trajectories when going from a space-fixed description to a body-fixed description.

The inelastic process of intramultiplet mixing (also referred to as fine-structure changing collisions), mediated by radial coupling at the ‘‘avoided crossings’’ in the adiabatic potentials, is incorporated in our semiclassical model with Landau-Zener theory.^{20,21,25,49} For each trajectory a crossing probability p_x is calculated for going to another Ne^{**} state of the $(3p)$ multiplet. At the crossing radius R_x the Ne^{**} $(3p)$ state is divided over the two states according to this probability. The particle trajectory thus splits into two trajectories when passing an avoided crossing. We have tested our semiclassical program by comparison with fully quantum-mechanical coupled-channel calculations²⁵ for the case of intramultiplet mixing in the Ne^{**}-He system (where, of course, ionization does not occur). We observe a very good agreement, both for absolute values and polarization effects. In our calculations for the Ne^{**} $[(3p); J=3]$ -Ar system, the radial coupling to the neighboring Ne^{**} $(3p)$ states is taken into account as well. We thus expect no difference between

our calculations and the calculations of Bussert *et al.*¹¹⁻¹³

The process of ionization for each $|J, \Omega\rangle$ state is described by the attenuation factor $\exp[-\Gamma_{\Omega}(R)\Delta t/\hbar]$. We thus obtain an ionization probability $P(b|J, M)$ for an initial pure magnetic substate Ne^{**} $(|J, M\rangle_g)$ colliding with an Ar atom with an impact parameter b . The total ionization cross section ${}^JQ^{|M|}$ can now be calculated through

$${}^JQ^{|M|} = \int_0^{\infty} db 2\pi b P(b|J, M). \quad (53)$$

A final remark concerns the absolute value of the autoionization width. In contrast to the simple one-electron model discussed by Driessen *et al.*,²¹ the two-electron approach of this paper should give absolute values. However, in the calculation of the two-center two-electron integrals of Eq. (23) with the ATMOL program the electron wave functions are scaled with a nonspecified normalization procedure. We were not able to deduce the relation of the normalization constant with the c_i and α_i coefficients of Eq. (22). Therefore we were forced to introduce an arbitrary scaling factor for the two-electron approximation. In Tables VI and VII we have tabulated the scaled autoionization widths $\Gamma_{\Omega}(R)$ which have been used in the semiclassical calculations.

B. Cross-section results for Ne^{**} $({}^3D_3)$ -Ar

For the Ne^{**} $({}^3D_3)$ -Ar system four independent polarized-atom cross sections ${}^3Q^{|M|}(E)$ are to be determined. Experimentally it is very difficult to prepare pure magnetic substates Ne^{**} $({}^3D_3, |J, M\rangle_g)$ with respect to the initial relative velocity g , thus one obtains experimental cross sections ${}^3Q^{|M|}(E)$ which are interdependent.^{11-13,20,21,48} To remove this interdependence we have determined the average cross sections

$$\begin{aligned} {}^3Q^{0,1} &= \frac{1}{3}({}^3Q^0 + 2{}^3Q^1) \quad \text{for } |M|=0, 1, \\ {}^3Q^{2,3} &= \frac{1}{2}({}^3Q^2 + {}^3Q^3) \quad \text{for } |M|=2, 3, \end{aligned} \quad (54)$$

which can be obtained with great accuracy.^{20,21,48} The observed polarization effect

$$\mathcal{R}(E) = {}^3Q^{0,1}(E) / {}^3Q^{2,3}(E) \quad (55)$$

shows a strong energy dependence. In the thermal energy range ($50 \text{ meV} \leq E \leq 150 \text{ meV}$) the polarization effect is pronounced ($\mathcal{R} \approx 1.6$) while in the superthermal range ($1000 \text{ meV} \leq E \leq 5000 \text{ meV}$) the effect nearly vanishes ($\mathcal{R} \approx 1$).

In Table VIII the semiclassical results are presented for both the average ionization cross section ${}^3Q(E)$ as well as the polarization effect $\mathcal{R}(E)$. We conclude that the energy dependence of the absolute cross-section value is best reproduced in the two-electron approximation. Both the one-electron approximation and the two-electron approximation reproduce the energy dependence of the polarization effect very well. The fine-structure branching ratio of the ionization cross section has been determined in the two-electron approximation as well. The results are in

good agreement with the experimental value at $E = 110$ meV of Bussert *et al.*,^{12,13} as shown in Table VIII.

C. Cross-section results for Ne*($^3P_0, ^3P_2$)-Ar

For the Ne*($^3P_0, ^3P_2$)-Ar system state-selected ionization cross sections have been measured,^{7,14-16,18} resulting in a ratio $Q(J=0)/Q(J=2)$ with a strong energy dependence $Q(J=0)/Q(J=2) \simeq 1.3$ at $E = 100$ meV increasing to $Q(J=0)/Q(J=2) \simeq 1.8$ at $E = 2500$ meV. The polarization effect ${}^2Q^{|M|}(E)$ for the Ne*($|J=2, M\rangle_g$)-Ar system has been determined by Bregel *et al.*¹⁴ and by Driessen *et al.*⁴⁸ The experimental results show a strong energy dependence of the polarization effect

$$\mathcal{R}(E) = {}^2Q^{0,1}(E)/{}^2Q^2(E). \quad (56)$$

At $E = 100$ meV we have $\mathcal{R} \simeq 1.3$, which decreases with increasing energy to $\mathcal{R} \simeq 0.8$ at $E = 2500$ meV.

In Table IX the semiclassical results for the Ne*($^3P_0, ^3P_2$)-Ar system are presented. The energy dependence of the ionization cross section $Q(J=0)$ is reproduced fairly well in the two-electron approximation while the simple one-electron model of Driessen *et al.*²¹ gives much too small absolute values at high collision en-

ergies. The experimental ratio $Q(J=0)/Q(J=2)$ shows a strong increase with increasing collision energy while the calculated ratio indicates the opposite behavior. Moreover, the calculated ratios are too small.

Furthermore, we observe that the calculated polarization effect $\mathcal{R}(E)$ is not as pronounced as the experimental results, but the energy dependence shows the same trend. In the two-electron approximation we have calculated the fine-structure branching ratio ${}^J B$ as well, which can be compared to experimental data of Bussert *et al.*,^{12,13} measured at a collision energy of $E = 60$ meV. The agreement is good for Ne*(3P_2)-Ar. For Ne*(3P_0)-Ar, however, the calculated fine-structure branching ratio is larger than the experimental results. This is due to the much stronger sensitivity of ${}^0 B$ to the difference of the calculated ratio of the two-center two-electron integrals c/a with Morgner's value²² derived from the experimental results for the final-state fine-structure branching ratio, as discussed in detail in Sec. III C.

VI. CONCLUDING REMARKS

Collision experiments with polarized laser-excited atoms have received an extensive amount of attention.

TABLE VIII. Semiclassical results for the average ionization cross section ${}^3Q(E)$ and the polarization effect ${}^3Q^{0,1}/{}^3Q^{2,3}$ as a function of the collision energy E in comparison with the experimental results using the two-electron approximation $\Gamma_{J',J\Omega}(R)$ [Eq. (28)] as input. The number in parentheses is the error in the last digit given. For comparison we also give the results of Driessen *et al.* (Ref. 21), obtained with a one-electron approximation autoionization width.

E (eV)	Expt. (a)	${}^3Q(E)$ (\AA^2)	
		(a)	Semiclassical This work
0.075	24.5	32.3	25.8
0.125	23.2	28.3	23.6
0.200	21.5	23.4	22.1
0.500		19.7	20.6
1.000	20.2	16.1	19.4
2.500	16.3	12.5	17.4

E (eV)	$\mathcal{R}(E) = {}^3Q^{0,1}(E)/{}^3Q^{2,3}(E)$		${}^3Q(3/2)/{}^3Q(1/2)$	
	Expt. (a)	(b)	Semiclassical (a)	Expt. (c)
0.075	1.59(6)	1.66(8)	1.62	1.59
0.110			1.69	11.60(3)
0.125	1.77(7)	1.70(6)	1.63	1.51
0.200	1.52(5)	1.62(3)	1.62	1.47
0.500			1.44	1.31
1.000	1.15(4)	1.05(11)	1.21	1.38
2.500	1.00(3)	0.96(11)	0.97	1.44

^aDriessen *et al.*, Ref. 21.

^bDriessen *et al.*, Ref. 48.

^cBussert *et al.*, Refs. 12 and 13.

TABLE IX. Semiclassical results for the average ionization cross section ${}^0Q(E)$ and ${}^2Q(E)$ and the polarization effect ${}^2Q^{0,1}/{}^2Q^2$ as a function of the collision energy E in comparison with the experimental results using the two-electron approximation $\Gamma_{J',J\Omega}(R)$ [Eq. (28)] as input. The number in parentheses is the error in the last digit given. For comparison we also give the results of Driessen *et al.* (Ref. 21), obtained with a one-electron approximation for the autoionization width.

E (eV)	Expt. (a)	${}^0Q(E)$ (\AA^2)		Expt. (a)	${}^0Q/{}^2Q$	
		(b)	Semiclassical This work		(b)	Semiclassical This work
0.075	21.6	21.1	23.1	1.27	1.11	1.15
0.125	26.9	22.5	27.6	1.34	1.13	1.12
0.200	30.8	22.4	29.6	1.41	1.12	1.09
1.000	33.4	17.4	30.7	1.66	1.08	1.06
2.500	29.0	13.4	29.3	1.76	1.04	1.05

E (eV)	Expt. (c)	$\mathcal{R} = {}^2Q^{0,1}/{}^2Q^2$		Expt. (d)	Fine-structure branching ratio ${}^JQ(3/2)/{}^JQ(1/2)$	
		(b)	Semiclassical This work		Ne*(3P_0) Semiclassical This work	Ne*(3P_2) Expt. (d)
0.060				3.94(14)		1.51(7)
0.075	1.43(5)	1.18	1.10		8.9	1.42
0.125	1.30(3)	1.07	0.93		10.5	1.60
0.200	1.42(6)	0.97	0.88		11.9	1.70
1.000	1.05(6)	0.88	0.88		16.9	1.76
2.500	0.82(7)	0.86	0.89		20.3	1.72

^aVerheijen and Beijerinck, Ref. 16.

^bDriessen *et al.*, Ref. 21.

^cDriessen *et al.*, Ref. 48.

^dHotop, Lorentzen, and Zastrow, Ref. 7.

Large polarization effects in the ionization cross section for the $\text{Ne}^{**}(3p)$ -rare-gas systems are observed. The interpretation of this polarization effect in terms of suitable Ω -dependent optical potentials is the original motivation for performing an *ab initio* calculation of the autoionization widths $\Gamma_{J\Omega}(R)$ for the $\text{Ne}^{**(*)}$ -Ar systems. Following Bieniek³⁴ and Jones and Dahler³⁶ we investigated the theory of the process of ionization within the framework of the Feshbach projection-operator formalism, with the discrete fine-structure states (before ionization) and the continuum states (after ionization) as spanning the two separate subspaces of Hilbert space. The autoionization widths are expressed in terms of coupling matrix elements, which are in general two-center n -electron integrals. We assume that only two electrons play an active role in this process and that all other electrons are "frozen." For the initial state these electrons are the Ar($3p$) core electron and the $\text{Ne}^{**(*)}(3s/3p)$ valence electron; in the final state the free electron is described by a Coulomb wave function with respect to Ar^+ while the bound electron is associated with a Ne($2p$) core orbital. Most important for Ne^* -Ar is the exchange mechanism, where simultaneously the Ar($3p$) electron jumps to the

$\text{Ne}^*(2p)^{-1}$ hole and the $\text{Ne}^*(3s)$ valence electron becomes a free electron. The radiative mechanism does not contribute in pure triplet states, due to spin-selection rules.

With the obtained Ω -dependent autoionization widths we have calculated polarized-atom cross sections ${}^JQ^{|M|}$ using a semiclassical model. For the $\text{Ne}^{**}({}^3D_3)$ -Ar system we observe a good agreement with the experimental data, if the effect of "locking" of the total angular momentum J to the internuclear axis is taken into account.

For the $\text{Ne}^*({}^3P_0, {}^3P_2)$ -Ar system, the agreement is less satisfying. Especially, the large cross-section ratio $Q({}^3P_0)/Q({}^3P_2)$ is not explained by our autoionization widths. It is clear that there is no simple answer to this problem. The semiclassical treatment of the collision dynamics for the $\text{Ne}^*({}^3P_{0,2})$ -Ar system is fully justified, as supported by the good agreement between experiment and theory for the $\text{Ne}^{**}({}^3D_3)$ -Ar system with its much larger Ω splitting of the potential. Concerning the calculation of the autoionization widths, the "local approximation" should be quite correct for the thermal energy range when looking at the criteria given by Morgner.⁴⁰

For the superthermal energy range the local approximation is no longer justified, with $E_{\text{ion,max}}/E \simeq 0.4$ (or 0.7 when the Rydberg states of Ar^+ are included⁴⁰), which should be compared to the criterion $E_{\text{ion,max}}/E \geq 2$ of Morgner.⁴⁰ The parameter $E_{\text{ion,max}}$ is the maximum kinetic energy of the ion in the final state. The last possibility is the replacement of the molecular $\text{Ne}^*\text{-Ar}$ states by their atomic equivalent. Because the coupling matrix elements are combined coherently, an analysis with the molecular $\text{Ne}^*\text{-Ar}$ states may result in slightly different autoionization widths which can explain the cross-section ratio $Q(^3P_0)/Q(^3P_2)$. In view of the observation by Bussert¹³ that at $R = 5.5a_0$ the adiabatic eigenstates for $\text{Ne}^{(*)}\text{-Ar}$ are still for 97% atomic states, we do not expect a very large influence. Especially at thermal energy, where internuclear distances $R > 6a_0$ are probed, the effect on the ionization cross section will be rather small. This leaves us at a loss for a final explanation of the ratio $Q(^3P_0)/Q(^3P_2)$ in the thermal energy range.

ACKNOWLEDGMENTS

This work is supported by the Foundation for Fundamental Research on Matter (FOM). The computer time (approximately 4 h) on the CYBER 205 was granted to us by the Foundation for University Computer Facilities (SURF).

APPENDIX:

AUTOIONIZATION WIDTH $\Gamma_{J',J\Omega}(R)$

The autoionization width $\Gamma_i(R)$ of Eq. (15) contains the two-center n -electron integrals $V(R; \Omega f q, i)$ of Eq. (12),

$$\begin{aligned} V(R; \Omega f q, i) &= \langle \phi_{\Omega f q} | H_{\text{el}} | \phi_{\Omega i} \rangle \\ &= \int d\mathbf{r}_n \phi_{q\lambda\mu}(\mathbf{r}_1 | \mathbf{R}) \phi_{\Omega, J' J}(\mathbf{r}_{n-1} | \mathbf{R}) \\ &\quad \times H_{\text{el}} \phi_{\Omega i}(\mathbf{r} | \mathbf{R}). \end{aligned} \quad (\text{A1})$$

We want to obtain an expression for $\Gamma_{J',J\Omega}(R)$, which resolves both the initial magnetic substate $\text{Ne}^{(*)}(|J, M\rangle_{\mathbf{R}})$ and the final fine-structure state $\text{Ar}^+(J')$. In order to derive this expression we make the assumption that the molecular $\text{Ne}^{(*)}\text{-Ar}$ states are given by (antisymmetrized) products of the atomic $\text{Ne}^{(*)}$ and Ar states.

The complicated bookkeeping due to the antisymmetrized nature of the initial and final states is dealt with automatically by using second quantization, i.e., by writing both of these states as linear combinations of products of creation operators for each of the total number of 28 electrons. The matrix element is even more conveniently calculated, however, by applying the second-quantization formalism in its particle-hole version.⁴⁷ We thus have

$$\begin{aligned} V(R; \Omega f q, i) &= V^{\text{exch}}(R; f = J' \Omega_I \lambda \mu m_s q, i = J \Omega) \\ &= \sum_{M_L M_S} (L M_L S M_S | J \Omega) \sum_{m_{l,c} m_{l,v}} (-1)^{1-m_{l,c}} (1 - m_{l,c} l_v m_{l,v} | L M_L) \\ &\quad \times \sum_{m_{s,c} m_{s,v}} (-1)^{1/2 - m_{s,c}} (\frac{1}{2} - m_{s,c} \frac{1}{2} m_{s,v} | S M_S) \\ &\quad \times \sum_{m_{l,\text{Ar}} m_{s,\text{Ar}}} (-1)^{1-m_{l,\text{Ar}}} (-1)^{1/2 - m_{s,\text{Ar}}} (1 - m_{l,\text{Ar}} \frac{1}{2} - m_{s,\text{Ar}} | J' \Omega_I) \\ &\quad \times \langle \lambda \mu m_s; 2p m_{l,c} m_{s,c} | H_{\text{el}} | l_v m_{l,v} m_{s,v}; 3p m_{l,\text{Ar}} m_{s,\text{Ar}} \rangle. \end{aligned} \quad (\text{A2})$$

As stated already in Sec. III B, the quantum numbers $(m_{l,c} m_{s,c})$ and $(m_{l,\text{Ar}} m_{s,\text{Ar}})$ refer to the electronic states $\text{Ne}(2p)$ and $\text{Ar}(3p)$, respectively, which are involved in the ionization process [see Eq. (23)]. The core states $\text{Ne}(2p)^{-1}$ and $\text{Ar}(3p)^{-1}$ are therefore described by the inverse m quantum numbers. The phase factors $(-1)^{l-m}$ result from inserting Eq. (26) into Eq. (25). According to Eq. (18) the matrix element in Eq. (A2) can be written as

$$\begin{aligned} \langle \lambda \mu m_s; 2p m_{l,c} m_{s,c} | H_{\text{el}} | l_v m_{l,v} m_{s,v}; 3p m_{l,\text{Ar}} m_{s,\text{Ar}} \rangle &= [V^{\text{exch}}(R; q \lambda \mu m_{l,c} m_{l,v} m_{l,\text{Ar}}) \langle \frac{1}{2} m_s | \frac{1}{2} m_{s,v} \rangle \langle \frac{1}{2} m_{s,c} | \frac{1}{2} m_{s,\text{Ar}} \rangle \\ &\quad - V^{\text{rad}}(R; q \lambda \mu m_{l,c} m_{l,v} m_{l,\text{Ar}}) \langle \frac{1}{2} m_s | \frac{1}{2} m_{s,\text{Ar}} \rangle \langle \frac{1}{2} m_{s,c} | \frac{1}{2} m_{s,v} \rangle]. \end{aligned} \quad (\text{A3})$$

The radiative part thus contains a term $\langle \frac{1}{2} m_{s,c} | \frac{1}{2} m_{s,v} \rangle$, which results in a Kronecker delta $\delta_{m_{s,c} m_{s,v}}$. The summation over $m_{s,v}$ and $m_{s,c}$ reduces to

$$\sum_{m_{s,c}} (\frac{1}{2} m_{s,c} \frac{1}{2} - m_{s,c} | S M_S) = \delta_{S,0} \delta_{M_S,0} \sqrt{2}. \quad (\text{A4})$$

Clearly, the radiative mechanism contributes only if the initial $\text{Ne}^{(*)}$ state is in a singlet state. This is easily understood: in a sense the decay of the $\text{Ne}^{(*)}$ state is an electric dipole decay involving a virtual photon which ionizes the Ar atom. In an electron dipole transition, however, no spin flip occurs.

Because the $\text{Ne}^{*(*)}$ states we are interested in are pure triplet states, only the exchange mechanism contributes to the autoionization widths. Therefore we can rewrite the transition matrix element of Eq. (A2), using the Kronecker deltas $\delta_{m_s, m_{s,v}}$ and $\delta_{m_{s,c}, m_{s,Ar}}$ in the matrix element $V^{\text{exch}}(R; f=J'\Omega_I \lambda \mu m_s q, i=J\Omega)$:

$$\begin{aligned} V^{\text{exch}}(R; f=J'\Omega_I \lambda \mu m_s q, i=J\Omega) &= \sum_{M_L} \sum_{M_S} (L M_L S M_S | J \Omega) \sum_{m_{l,c}} \sum_{m_{l,v}} (-1)^{1-m_{l,c}} (1-m_{l,c}) J_v m_{l,v} | L M_L) \\ &\times \sum_{m_{s,c}} \sum_{m_{s,v}} (-1)^{1/2-m_{s,c}} \left(\frac{1}{2}-m_{s,c}\right) \left(\frac{1}{2}m_{s,v}\right) | S M_S) \\ &\times \sum_{m_{l,Ar}} \sum_{m_{s,Ar}} (-1)^{1-m_{l,Ar}} (-1)^{1/2-m_{s,Ar}} (1-m_{l,Ar})^{1/2} (1-m_{s,Ar}) | J' \Omega_I) \\ &\times \int d\mathbf{r}_1 d\mathbf{r}_2 \psi_{q\lambda\mu}^{Ar}(\mathbf{r}_1) \psi_{2p, m_{l,c}}^{\text{Ne}}(\mathbf{r}_2) \frac{e^2}{4\pi\epsilon_0 |\mathbf{r}_1 - \mathbf{r}_2|} \\ &\times \psi_{3s/3p, m_{l,v}}^{\text{Ne}}(\mathbf{r}_1) \psi_{3p, m_{l,Ar}}^{Ar}(\mathbf{r}_2). \end{aligned} \quad (\text{A5})$$

The final expression we obtain for the autoionization width $\Gamma_{J', J\Omega}(R)$ according to Eq. (15) is given by

$$\Gamma_{J', J\Omega}(R) = \frac{2\pi m_e}{\hbar^2 q(R)} \sum_{\Omega_I} \sum_{\lambda} \sum_{\mu, m_s} |V^{\text{exch}}(R; f=J'\Omega_I \lambda \mu m_s q, i=J\Omega)|^2. \quad (\text{A6})$$

*Present address: Joint Institute for Laboratory Astrophysics, Boulder, CO 80309-0440.

¹S. Y. Tang, A. B. Marcus, and E. E. Muschlitz, Jr., *J. Chem. Phys.* **56**, 566 (1972).

²E. Illenberger and A. Niehaus, *Z. Phys. B* **20**, 33 (1975).

³W. P. West, T. B. Cook, F. B. Dunning, R. D. Dundel, and R. F. Stebbings, *J. Chem. Phys.* **63**, 1237 (1975).

⁴A. Pesnelle, G. Watel, and C. Manus, *J. Chem. Phys.* **62**, 3590 (1975).

⁵R. H. Neynaber and G. D. Magnuson, *Phys. Rev. A* **11**, 865 (1975).

⁶M. R. Woodard, R. C. Sharp, M. Seeley, and E. E. Muschlitz, Jr., *J. Chem. Phys.* **69**, 2978 (1978).

⁷H. Hotop, J. Lorentzen, and Z. Zastrow, *J. Electron. Spectrosc. Relat. Phenom.* **23**, 347 (1981).

⁸A. Niehaus, in *The Excited State in Chemical Physics*, edited by J. Wm. McGowan (Wiley, New York, 1981), Chap. 2.

⁹R. W. Gregor and P. E. Siska, *J. Chem. Phys.* **74**, 1078 (1981).

¹⁰T. P. Parr, D. M. Parr, and R. M. Martin, *J. Chem. Phys.* **76**, 316 (1982).

¹¹W. Bussert, T. Bregel, J. Ganz, K. Harth, A. Siegel, M. W. Ruf, H. Hotop, and H. Morgner, *J. Phys. (Paris) Colloq.* **45**, C1-199 (1984).

¹²W. Bussert, T. Bregel, R. J. Allan, M. W. Ruf, and H. Hotop, *Z. Phys. A* **320**, 105 (1985).

¹³W. Bussert, Ph.D. thesis, Universität Kaiserslautern, Germany, 1985.

¹⁴T. Bregel *et al.*, in *Electronic and Atomic Collisions*, edited by D. C. Lorents, W. E. Meyerhof, and J. R. Peterson (North-Holland, Amsterdam, 1986), p. 577.

¹⁵C. Weiser and P. E. Siska, *J. Chem. Phys.* **85**, 4746 (1986).

¹⁶M. J. Verheijen and H. C. W. Beijerinck, *Chem. Phys.* **102**, 255 (1986).

¹⁷J. P. C. Kroon, A. Cottaar Haverkorn, and H. C. W. Beijerinck, *Chem. Phys.* **103**, 119 (1986).

¹⁸F. T. M. van den Berg, J. H. M. Schonenberg, and H. C. W. Beijerinck, *Chem. Phys.* **115**, 359 (1987).

¹⁹H. A. J. Meijer, T. J. C. Pelgrim, H. G. M. Heideman, R. Morgenstern, and N. Anderson, *Phys. Rev. Lett.* **59**, 2939 (1987); *J. Chem. Phys.* **90**, 738 (1989).

²⁰J. P. J. Driessen, F. J. M. van de Weijer, M. J. Zonneveld, L. M. T. Somers, M. F. M. Janssens, H. C. W. Beijerinck, and B. J. Verhaar, *Phys. Rev. Lett.* **62**, 2369 (1989).

²¹J. P. J. Driessen, F. J. M. van de Weijer, M. J. Zonneveld, L. M. T. Somers, M. F. M. Janssens, H. C. W. Beijerinck, and B. J. Verhaar, *Phys. Rev. A* **42**, 4058 (1990).

²²H. Morgner, *J. Phys. B* **18**, 251 (1985).

²³D. Hausamann, Ph.D. thesis, Albert-Ludwigs-Universität, Freiburg, Germany, 1985.

²⁴M. P. I. Manders, J. P. J. Driessen, H. C. W. Beijerinck, and B. J. Verhaar, *Phys. Rev. Lett.* **57**, 1577 (1986); **57**, 2472 (1986); *Phys. Rev. A* **37**, 3237 (1988).

²⁵M. P. I. Manders, W. B. M. van Hoek, E. J. D. Vredenburg, G. J. Sandker, H. C. W. Beijerinck, and B. J. Verhaar, *Phys. Rev. A* **39**, 4467 (1989).

²⁶F. Masnou-Seeuws, M. Philippe, and P. Valiron, *Phys. Rev. Lett.* **41**, 95 (1978).

²⁷D. Hennecart and F. Masnou-Seeuws, *J. Phys. B* **18**, 657 (1985).

²⁸D. Hausamann and H. Morgner, *Mol. Phys.* **54**, 1085 (1985).

²⁹H. Hotop and A. Niehaus, *Z. Phys.* **228**, 68 (1969).

³⁰W. H. Miller and H. Morgner, *J. Chem. Phys.* **67**, 4923 (1977).

³¹K. T. Gillen, P. R. Jones, and T. Tsuboi, *Phys. Rev. Lett.* **56**, 2610 (1986).

³²H. Feschbach, *Ann. Phys. (N.Y.)* **19**, 287 (1962).

³³T. F. O'Malley, *Phys. Rev.* **150**, 14 (1966); **156**, 230 (1967).

³⁴R. J. Bieniek, *Phys. Rev. A* **18**, 392 (1978).

³⁵A. P. Hickman, A. D. Isaacson, and W. H. Miller, *J. Chem. Phys.* **66**, 1483 (1977).

³⁶D. M. Jones and J. S. Dahler, *Phys. Rev. A* **37**, 2916 (1988).

³⁷W. H. Miller, C. A. Slocumb, and H. F. Schaefer III, *J. Chem. Phys.* **56**, 1347 (1972).

³⁸H. P. Saha, J. S. Dahler, and S. E. Nielsen, *Phys. Rev. A* **28**, 1487 (1983).

- ³⁹S. E. Haywood and J. B. Delos, *Chem. Phys.* **145**, 253 (1990).
- ⁴⁰H. Morgner, *Chem. Phys.* **145**, 239 (1990).
- ⁴¹E. Clementi, *IBM J. Res. Dev. Suppl.* **9**, 2 (1965).
- ⁴²H. Haberland (private communication).
- ⁴³M. Aymar, S. Feneuille, and M. Klapisch, *Nucl. Instrum. Methods* **90**, 137 (1970).
- ⁴⁴H. Kucal, D. Hennecart, and F. Masnou-Seeuws, *Z. Phys. D* **13**, 241 (1989).
- ⁴⁵D. Moncrief and V. R. Saunders, in *ATMOL Manual*, edited by R. Scott Huxley, University of Manchester, Regional Computer Centre, Manchester, England, 1986 (unpublished).
- ⁴⁶V. R. Saunders, in *Methods in Computational Molecular Physics*, edited by G. H. F. Dierksen and S. Wilson (Reidel, Dordrecht, 1983), p. 1.
- ⁴⁷P. J. Brussaard and P. W. M. Glaudemans, *Shell-Model Applications in Nuclear Spectroscopy* (North-Holland, Amsterdam, 1977), Chap. 13.
- ⁴⁸J. P. J. Driessen, H. J. L. Megens, M. J. Zonneveld, H. A. J. Senhorst, H. C. W. Beijerinck, and B. J. Verhaar, *Chem. Phys.* **147**, 447 (1990).
- ⁴⁹E. E. Nikitin, in *Chemische Elementar Prozesse*, edited by H. Hartmann and J. Heidelberg (Springer-Verlag, Heidelberg, 1968).